PERGAMON

Deep-Sea Research II 49 (2002) 1645–1674

DEEP-SEA RESEARCH
PART II

www.elsevier.com/locate/dsr2

Vertical budgets for organic carbon and biogenic silica in the Pacific sector of the Southern Ocean, 1996–1998

David M. Nelson[a,*], Robert F. Anderson[b], Richard T. Barber[c], Mark A. Brzezinski[d], Ken O. Buesseler[e], Zanna Chase[b,1], Robert W. Collier[a], Mary-Lynn Dickson[f], Roger François[e], Michael R. Hiscock[c], Susumu Honjo[e], John Marra[b], William R. Martin[e], Raymond N. Sambrotto[b], Frederick L. Sayles[e], Daniel E. Sigmon[a]

[a] *College of Oceanic and Atmospheric Sciences, Oregon State University, Corvallis, OR 97331, USA*
[b] *Lamont-Doherty Earth Observatory, Columbia University, Palisades, NY 10964, USA*
[c] *Duke University Marine Laboratory, Beaufort, NC 28516, USA*
[d] *Department of Ecology, Evolution & Marine Biology, University of California, Santa Barbara, CA 93106, USA*
[e] *Woods Hole Oceanographic Institution, Woods Hole, MA 02543, USA*
[f] *Graduate School of Oceanography, University of Rhode Island, Narragansett, RI 02882, USA*

Abstract

During the 1996–1998 Antarctic Environment and Southern Ocean Process Study (AESOPS), a component of US JGOFS, we obtained seasonal or longer-term data sets on the rates of production, vertical transport, remineralization and burial of particulate organic carbon (POC) and biogenic silica ($BSiO_2$) in the Southern Ocean at 170°W between 55°S and 68°S. The AESOPS data records enable us to construct vertical C and Si budgets for the water column and upper sediments, with all estimates derived from direct measurement of the relevant fluxes.

We constructed annual C and Si budgets for each of four ecologically distinct zonal bands within the system. For both POC and $BSiO_2$ the greatest annual delivery to the sea floor ($\sim$200 and 1400 mmol m^{-2} yr^{-1}, respectively) and burial ($\sim$6 and 160 mmol m^{-2} yr^{-1}, respectively) were observed in the southern Antarctic Circumpolar Current (ACC) between 61.5°S and 65.5°S. That pattern is consistent with our observation that a diatom bloom propagated southward through the southern ACC during the spring and summer of 1997–1998, following the receding ice edge, and that this bloom was the main source of both POC and $BSiO_2$ in the system on an annual basis. In the other zones the annual fluxes of POC and $BSiO_2$ to the sea floor ranged from 19% to 67% of those in the zone traversed by the summer diatom bloom. The higher benthic fluxes of both POC and $BSiO_2$ in the southern ACC imply that blooms similar to the one we observed in 1997–1998 occur commonly in the southern ACC, and that their high-productivity signature is transmitted to the sea floor.

The data show preferential preservation of $BSiO_2$ over POC throughout the water column and upper seabed. In the four zonal bands we consider, $BSiO_2$ and POC are produced in mole ratios of 0.1–0.4, exported from the upper 100 m in ratios of 0.2–0.6, arrive at 1000 m in ratios of 1.5–4.5, reach the sea floor in ratios of 2.2–7.6, and are buried in ratios of 11.6–28. Despite the preferential preservation of $BSiO_2$, accumulation of opal-rich sediments beneath the ACC does not result from unusually efficient preservation of siliceous material. The estimated $BSiO_2$ preservation efficiency

*Corresponding author. Fax: +1-541-737-2064.
E-mail address: nelsonda@coas.oregonstate.edu (D.M. Nelson).
[1] Present address: Monterey Bay Aquarium Research Institute, Moss Landing, CA 95039, USA.

0967-0645/02/$ - see front matter © 2002 Elsevier Science Ltd. All rights reserved.
PII: S0967-0645(02)00005-X

(burial-production) ranges from 1.2% to 5.5%, indistinguishable from the global average of 3%. Instead, opal-rich sediment accumulation in this region reflects very high annual rates of $BSiO_2$ production in surface waters, along with very low accumulation rates of other sedimentary components (e.g., $CaCO_3$ and detrital material).

The observed high ratios of $BSiO_2$ production to POC production in surface waters are consistent with the known tendency for the Si/C ratio of diatoms to increase when [Fe] is low. If greater Fe availability during the last glacial maximum permitted diatoms in the Southern Ocean to grow with lower, more normal Si/C ratios, export of diatom-produced POC could have occurred at 2–3 times its present rate. A corresponding increase in opal export or opal sediment accumulation is unlikely because silicic acid is almost totally depleted north of 65°S under present conditions. Thus, even large increases in POC production and export during glacial periods would not be reflected in the opal accumulation record. © 2002 Elsevier Science Ltd. All rights reserved.

Résumé

Dans le cadre du programmme AESOPS/US-JGOFS une étude de processus a été menée de 1996 à 1998 dans le secteur Pacifique de l'Océan Austral (le long de 170°W). L'objectif est la détermination des flux annuels et des variations saisonnières de la production primaire dans la couche de surface, du flux vertical du carbone organique particulaire (POC) et de la silice biogène ($BSiO_2$) dans la colonne d'eau ainsi que des flux de recyclage des éléments biogènes. Quatre bandes zonales sont considérées de 55 à 68°S. Les flux de POC et de $BSiO_2$ les plus élevés sont mesurés dans la bande zonale sud du Courant Antarctique Circumpolaire (ACC), de 61,5 à 65,5°S, où les floraisons de diatomées se déplaçent au printemps-été vers le sud, dans le sillage des glaces; au niveau de l'interface eau-sédiment les flux sont de 200 et 1400 mmole m^{-2} an^{-1} respectivement, les flux nets enfouis correspondant étant de 6 et 1600 mmole m^{-2} an^{-1}. Dans les autres bandes zonales les flux annuels à l'interface eau-sédiment ne représentent que 19 à 67% des valeurs observées dans la bande zonale précédente. Le fait de trouver des flux benthiques élevées dans la bande zonale sud du Courant Antarctique Circumpolaire indique que les sédiments de cette bande zonale sont régulièrement alimentés par des flux élevés de matière biogène.

Au cours du transport vertical la $BSiO_2$ est mieux préservée que le POC comme l'indique la variation des rapports molaire de silice et de carbone en fonction de la profondeur. Pour l'ensemble des quatre bandes zonales ces rapports passent de 0,1–0,4 pour la production dans la couche de surface à 0,2–0,6 pour la production exportée à 100 m. A 1000 m ils montent à 1,5–4,5, s'élèvent à 2,2–7,6 à l'interface eau-sédiment, et atteignent 11,6–28 dans les dépôts sédimentaires. En dépit de cette préservation privilégié de l'opale, même dans la bande zonale où les dépôts sédimentaires sont particulièrement riches en opale, le rapport de préservation (rapport du flux sédimentaire net sur le flux de production) n'est que de 1,2–5,5%, ce qui n'est pas significativement différent de la moyenne de 3% pour l'océan mondial. La richesse en opale des sédiments antarctiques s'explique donc non pas par une préservation d'opale exceptionnelle dans les sédiments mais par une production de silice biogène élevée dans la couche de surface, et ceci par rapport aux autres flux de matière biogène (carbonate de calcium et détritus) beaucoup plus limités.

Les rapports $BSiO_2$/ POC élevés mesurés dans le matériel planctonique des eaux de surface s'expliquent par l'impact d'un déficit en fer des eaux de surface sur la croissance des diatomées. Au dernier maximum glaciaire une plus grande disponibilité en fer dans la couche de surface de l'Océan Austral a du se traduire par des rapports Si/C dans le matériel exporté 2 à 3 fois plus faibles qu'actuellement. Ainsi il est peu probable qu'au dernier maximum glaciaire, même si les flux de POC étaient plus élevés que dans l'océan moderne, les flux de silice biogéne exportée aient été plus importants qu'actuellement, d'autant que la croissance des diatomées aunord de 65°S est limitée par la disponibilité en acide silicique.

1. Introduction

The Southern Ocean is the largest of several high-nutrient, low-chlorophyll (HNLC) regions in the world's oceans. This region plays a major role in regulating the global net transfer of carbon dioxide between the ocean and the atmosphere, in part because the annual photosynthetic uptake of CO_2 by phytoplankton and resulting export of particulate organic carbon (POC) to the deep ocean are significantly less than the available macronutrients nitrogen and phosphorus would sustain (e.g., Sarmiento et al., 1998). Changes in the efficiency of this "biological pump" (Volk and

Hoffert, 1985; Longhurst and Harrison, 1989) have been hypothesized to play a major role in regulating atmospheric CO_2 concentrations on glacial/interglacial time scales (Knox and McElroy, 1984; Martin, 1990; Moore et al., 2000).

The relatively low primary productivity of the Southern Ocean went unrecognized for decades. As recently as the mid 1970s global productivity maps showed either large regions or a broad circumpolar band within the Antarctic Circumpolar Current (ACC) where primary productivity was $>200\,g\ C\,m^{-2}\,yr^{-1}$ (e.g., Lieth, 1975). The perceived high productivity was based mainly on two lines of indirect evidence; the high biomass of seals, seabirds and other large carnivores in the region (Croxall and Prince, 1979; Brown and Lockyer, 1984) and the presence of diatom-rich siliceous sediments underlying much of the ACC (Goodell et al., 1973; DeMaster, 1981). However, the first large-scale ^{14}C productivity surveys in the ACC showed very low productivity throughout most of the region, even during the relatively short summer growing season (El-Sayed and Turner, 1975; Holm-Hansen et al., 1977). As a consequence, productivity estimates for the ACC were revised downward to as low as $16\,g\,C\,m^{-2}\,yr^{-1}$ (El-Sayed, 1978). Somewhat higher estimates were obtained by accounting for the effects of ice-edge phytoplankton blooms (Smith et al., 1988) and areas of high productivity near the Antarctic Polar Front (APF) (Laubischer et al., 1993), but no ^{14}C-based estimate has ever approached the $200\,g\,C\,m^{-2}\,yr^{-1}$ level estimated from indirect evidence. Subsequent estimates based on satellite ocean color, sea-surface temperature and irradiance data, applied to temperature-dependent photosynthesis/irradiance models (Antoine et al., 1996; Behrenfeld and Falkowski, 1997; Moore and Abbott, 2000), indicate primary productivity of $<50\,g\,C\,m^{-2}\,yr^{-1}$ throughout most of the ACC south of 55°S. That is less than half the annual productivity determined by ^{14}C uptake at time-series sites in the Sargasso Sea near Bermuda (Michaels et al., 1994) and North Pacific Central Gyre near Hawaii (Letelier et al., 1996), implying that most of the ACC is less productive on an annual basis than even the classically oligotrophic mid-ocean gyres.

The opal sediment record is the most obvious long-term signal emanating from biological processes in the ACC. Opal (hydrated amorphous silica, which in the Southern Ocean consists almost exclusively of diatom remains) comprises from ~50% to >90% (by weight) of modern abyssal sediments beneath the ACC (Broecker and Peng, 1982), making the region a major oceanic sink for Si (DeMaster, 1981; Tréguer et al., 1995). Subsequent estimates of opal burial rates beneath the ACC, using ^{230}Th-normalized accumulation rates to account for sediment focusing, have lowered the estimated burial rate by about a factor of two, but burial remains a major removal term in the global oceanic Si budget (DeMaster, 2002). Several recent studies have addressed what Pondaven et al. (2000) termed the "opal paradox" in the Southern Ocean: the accumulation of opal-rich diatom sediments in an area of low primary productivity. This accumulation has been hypothesized to result either from unusually efficient preservation of biogenic silica in the water column (Nelson et al., 1995) or from an unusually high production of biogenic silica in surface waters (e.g. Pondaven et al., 2000). Understanding the processes generating the opal sediments beneath the ACC is important in any attempt to reconstruct paleoproductivity patterns in the region. Do past changes in opal accumulation rates reflect changes in total primary productivity, in diatom productivity alone, in preservation efficiency, or in some combination of the three? Moreover, the organic carbon content of the sediments in the Southern Ocean is low, as is typical of many open-ocean environments (Van Bennekom et al., 1988; DeMaster et al., 1991). Are the cycles of carbon and silicon decoupled in the Southern Ocean to a degree that precludes use of the opal sediment record as an indicator of primary productivity or POC export to the deep sea, or can useful paleoproductivity information be derived from that record (e.g., Ragueneau et al., 2000)?

During the recently completed Antarctic Environment and Southern Ocean Process Study (AESOPS), a component of US JGOFS, we conducted a suite of biogeochemical studies focused on the cycles of C, N and Si in the Pacific sector of the ACC. Those studies were centered at

170°W and extended from ~53°S (well north of the APF) to ~71°S (well south of the Southern ACC Front (SACCF) and into the Ross Gyre). We thus obtained data across the full meridional extent of the ACC and from waters to the south. We measured fluxes (rates of production, remineralization and vertical transport) of organic carbon, organic nitrogen, and biogenic silica in surface waters, in the subsurface water column, and in the seabed between November 1996 and March 1998. We have reported on a number of those individual studies (Honjo et al., 2000; Sambrotto and Mace, 2000; Brzezinski et al., 2001; Buesseler et al., 2001; Nelson et al., 2001; Dickson and Orchardo, 2001; Sayles et al., 2001; Sigmon et al., 2002; see Table 1). Combining our data sets to estimate annual C and Si fluxes in the upper ocean, deep ocean, and seabed has enabled us to quantify most of the important features of the C and Si cycles in the system. In this paper we report those estimated annual fluxes, use them to construct vertical budgets for POC and biogenic silica ($BSiO_2$) and evaluate the quantitative relationships between the C and Si cycles throughout the water column and upper sediments. The results provide insights into the processes generating siliceous sediments in the region, and the likely changes in those processes on glacial/interglacial time scales

2. Methods

2.1. Study area and timing of observations

We collected samples and data in the Pacific sector of the Southern Ocean southeast of New Zealand during a series of cruises between November 1996 and March 1998 aboard the research vessels *Nathaniel B. Palmer* and *Roger Revelle*. Those cruises sampled almost entirely in the vicinity of 170°W, and extended from ~53°S to ~71°S (Fig. 1). In late November 1996 bottom-moored arrays of sediment traps were deployed from the *Palmer* along 170°W at the locations shown in Fig. 1. Bottom depths at those sites are given in Table 2. Traps on these arrays collected

Table 1
Experimental and analytical methods used, and papers presenting the individual data sets

Depth	Process	Method	Reference
A. Organic carbon data			
Euphotic zone	Gross photosynthesis	^{18}O conversion from H_2O to O_2	Dickson & Orchardo, 2001
Euphotic zone	Net community production	$d[O_2]/dt$	Dickson & Orchardo, 2001
Euphotic zone	POC production	^{14}C uptake	Barber & Marra, unpublished data
Euphotic zone	New production	$^{15}NO_3^-$ uptake	Sambrotto & Mace, 2000
50 m	New production	Seasonal NO_3^- drawdown	This paper
100 m	Particulate flux	^{234}Th deficit, > 70 μm POC	Buesseler et al., 2001
1,000 m	Particulate flux	Sediment trap collections	Honjo et al., 2000
Sea floor	Particulate rain	Remineralization + burial	This paper
Sea floor	Remineralization	Pore-water NO_3^-, TCO_2 & alkalinity profiles	Sayles et al., 2001
Sea floor	Long-term burial	^{230}Th-normalized accumulation	Sayles et al., 2001
B. Biogenic silica data			
Euphotic zone	Gross production	^{32}Si uptake	Brzezinski et al., 2001
50 m	Net production	Seasonal $Si(OH)_4$ drawdown	Sigmon et al., 2002
50 m	Export	Seasonal $(Si(OH)_4 + BSiO_2)$ drawdown	Sigmon et al., 2002
100 m	Particulate flux	^{234}Th deficit, > 70 μm $BSiO_2$	Buesseler et al., 2001
1,000 m	Particulate flux	Sediment trap collections	Honjo et al., 2000
Sea floor	Particulate rain	Remineralization plus burial	This paper
Sea floor	Remineralization	Pore-water $Si(OH)_4$ profiles	Sayles et al., 2001
Sea floor	Long-term burial	^{230}Th-normalized accumulation	Sayles et al., 2001

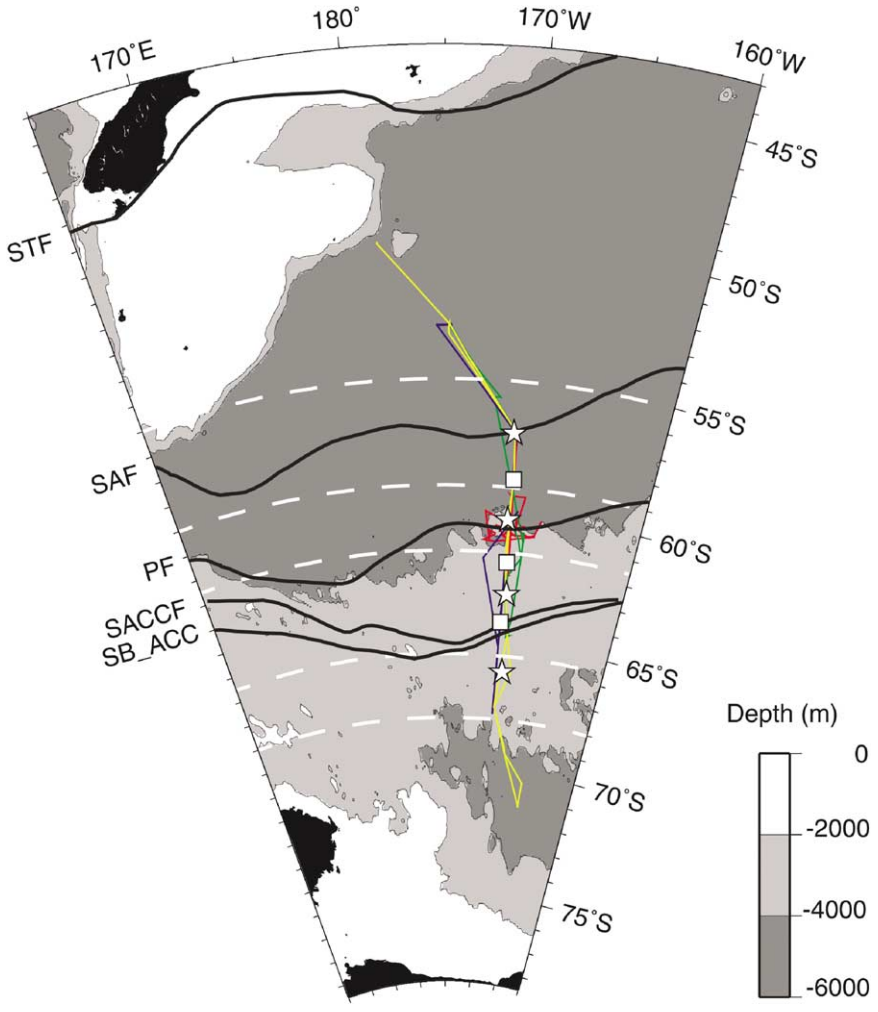

Fig. 1. The AESOPS study area, locations of main sampling sites and boundaries of sub-regions used for vertical budgets. Cruise tracks of the R./V. *Roger Revelle* in October/November 1997 are shown in red, November/December 1997 in green, January/February 1998 in blue and February/March 1998 in yellow. Gross production and net production of POC and $BSiO_2$ in the euphotic zone and export of both phases from the upper 100 m were measured along these cruise tracks over the time intervals shown in Table 2. Bottom-moored sediment traps were deployed from late November 1996 to mid January 1998 to measure the sinking fluxes of POC and $BSiO_2$ at the sites shown with stars. Benthic fluxes (remineralization and burial) of POC and $BSiO_2$ were also measured at the sites shown with stars, and at the additional sites shown with rectangles. White dashed lines denote the boundaries of the four sub-regions selected for vertical budgets based on data at ~170°W: the northern ACC (55°–59°S), polar frontal region (59°–61.5°S), southern ACC (61.5–65.5°S) and Ross Gyre (65.5°–68°S). Reasons for placing the boundaries at those latitudes at 170°W are discussed in the text. The mean positions of the Subtopical Front (STF), Subantarctic Front (SAF), PF, SACCF and southern boundary of the Antarctic Circumpolar Current (SB_ACC) in the study area (from Orsi et al., 1995) are shown with black solid lines.

samples for predetermined intervals of 8.5–136 days from the time of deployment until late January 1998. Details of the trap design and the full data set on POC and opal fluxes at all depths are given by Honjo et al. (2000). Each trap array included a programmable, interval-collecting trap at ~1000 m (937–1031 m) and the material collected in those traps forms the basis of the

Table 2
Time intervals over which rates of organic carbon and biogenic silica production were measured, latitudes and bottom depths of AESOPS sediment-trap mooring sites and benthic flux stations in the Southern Ocean

Sub-region	Northern ACC (55°–59 °S)	Polar Frontal Region (59°–61.5 °S)	Southern ACC (61.5°–65.5 °S)	Ross Gyre (65.5°–68 °S)
Time over which surface-layer rates were measured[1]				
Gross and net photosynthesis	Dec. 7–Feb. 19	Dec. 7–Feb. 21	Dec. 12–Mar. 10	—[3]
POC production	Dec. 7–Mar. 13	Nov. 1–Mar. 13	Oct 28–Mar. 10	Feb. 27–Mar. 7
New production	Dec. 7–Feb. 20	Dec. 11–Feb. 21	Dec. 16–Mar. 10	—[3]
$BSiO_2$ production	Dec. 6–Mar. 13	Nov. 2–Mar. 13	Oct. 29–Mar. 11	Jan. 16–Mar. 7
POC and $BSiO_2$ export[2]	Oct. 24–Feb. 18	Nov. 1–Feb. 21	Oct. 28–Mar. 10	Jan. 17–Feb. 27
Latitude of sediment-trap mooring site (°S)	56.88	60.27	63.17	66.14
Bottom depth at sediment-trap mooring site (m)	4,969	3,978	2,930	3,148
Latitudes of benthic flux sites (°S)	56.88, 58.69	60.27	61.88, 63.17, 64.20	66.14
Bottom depths at benthic flux sites (m)	4,969, 4,345	3,978	3,303, 2,930, 2,746	3,148

[1] During austral spring and summer, 1997–1998.
[2] Export estimates are based on ^{234}Th deficits, which integrate export over the 2–4 weeks prior to sampling.
[3] $H_2^{18}O$, $d[O_2]/dt$ and $^{15}NO_3^-$ incubation data in the Ross Gyre are insufficient to provide direct estimates of annual gross photosynthesis, net community production or new production.

estimated 1000-m settling fluxes reported here. We sampled from the *Palmer* to measure benthic remineralization and burial fluxes of organic carbon and biogenic silica at each of the four mooring sites where sediment traps were deployed, plus three other sites as shown in Fig. 1 and Table 2, during the mooring recovery cruise in February 1998 (Sayles et al., 2001).

We measured rates of organic matter and biogenic silica production in the euphotic zone and their export from the upper 100 m on a series of four cruises aboard the *Revelle* between late October 1997 and mid March 1998. Sampling on each cruise was also centered on 170°W, and extended from ~53°S to 63°–71°S, with the southward extent of sampling increasing as summer progressed and the sea ice retreated (Fig. 1). The first two cruises (in October/November and December/January) sampled southward to the edge of the retreating pack ice, which was located at ~63°S and ~65°S, respectively. The third and fourth cruises (in January and February/March) encountered no pack ice and sampled to ~68°S and ~71°S, respectively. We performed tracer incubation experiments with ^{18}O, ^{14}C, ^{15}N and ^{32}Si to measure rates of gross photosynthesis, POC production, NO_3^- uptake and $BSiO_2$ production within the euphotic zone at stations along these transect lines (Sambrotto and Mace, 2000; Brzezinski et al., 2001; Dickson and Orchardo, 2001) and incubation experiments to measure net community production from the change in dissolved $[O_2]$ with time (Dickson and Orchardo, 2001). Dates over which we obtained each of these data sets are presented in Table 2.

We also estimated seasonal net production of POC and $BSiO_2$ from the observed seasonal drawdown of nitrate and silicic acid in the upper 50 m. We estimated export of POC and $BSiO_2$ from the upper 100 m based on ^{234}Th deficits in the upper 100 m, in combination with the POC and $BSiO_2$ content of the >70 μm particles presumed to be the main agents of vertical transport in the system (Buesseler et al., 2001). The spatial extent of the combined measurements of ^{234}Th deficits and >70 μm POC and $BSiO_2$ was greatest on the cruises in December and February/March. Further details of the sampling locations and dates, and all measured rates of photosynthesis, nutrient uptake and biogenic particle export used in the budgets presented here, can be found at the US JGOFS website: http://usjgofs.whoi.edu/southern.html.

2.2. Rate measurements

The experimental and analytical methods used for measuring carbon and silica fluxes are summarized in Table 1, and are presented in detail in the separate papers reporting the original data sets (Honjo et al., 2000; Sambrotto and Mace, 2000; Brzezinski et al., 2001; Buesseler et al., 2001; Sayles et al. 2001; Dickson and Orchardo, 2001; Sigmon et al., 2002). We present the main features of those methods here, and refer the reader to the papers cited above for more complete descriptions.

Gross photosynthesis and net community production. We measured the gross rate of photosynthetic O_2 production by adding ^{18}O-labeled H_2O to seawater samples, incubating and measuring the production of ^{18}O-labeled dissolved O_2 (Bender et al., 1987). We determined net community production from changes in the concentration of dissolved O_2 during incubation experiments. For experiments of both kinds, we collected samples from depths corresponding to 85%, 50%, 25%, 18%, 10%, 5% and 1% of surface irradiance. Incubations were done on deck under natural sunlight, in incubators maintained at sea-surface temperature with running seawater and screened with combinations of blue and neutral-density photographic screening to achieve irradiance levels that simulated those in situ. All incubations began about 1 h before sunrise and lasted $\sim$24 h. Vertically integrated daily rates, in mmol $C\,m^{-2}\,d^{-1}$, were calculated by trapezoidal integration of the data. Due to an over-collection of incident radiation by the two incubators receiving the highest irradiance levels, data from those incubations were not included in the integrations. Instead, gross and net O_2 production rates were integrated by extending the production rate measured at the third optical depth (25% of surface irradiance) to the surface and integrating the rest of the profile to the 1% light level (Dickson and Orchardo, 2001). This modification of the integration scheme increased the calculated gross and net production by an average of 13% and 23%, respectively, in spring and by 1% and 34%, respectively, in summer over vertically integrated rates that do not correct for photoinhibition in incubations performed at higher-than-ambient light levels.

We converted the measured rates of O_2 production to carbon units using the equations:

$$\text{Net } C_{org} \text{ prod.} = (\text{Net } O_2 \text{ prod.}/1.4), \quad (1)$$

$$\text{Gross } C_{org} \text{ prod.} = \text{Net } C_{org} \text{ prod.} + ((\text{Gross } O_2 \text{ prod.} - \text{Net } O_2 \text{ prod.})/1.1), \quad (2)$$

where all production rates are expressed in mmol C or $O_2\,m^{-2}\,d^{-1}$. We applied a photosynthetic quotient (PQ) of 1.4 to the net O_2 production data and a PQ of 1.1 to the difference between gross O_2 and net O_2 production. The higher PQ assumes that nitrogen is obtained as nitrate, which must be reduced to be assimilated into organic matter, and the lower PQ on use of the regenerated nitrogenous nutrients ammonium and urea (Laws, 1991).

POC production. We measured the conversion of ^{14}C-labeled bicarbonate ($H^{14}CO_3^-$) to organic matter retained by glass-fiber filters (GFF; nominal pore size $\sim$0.7 μm) during $\sim$24-hr incubations. Depths sampled, incubation conditions and vertical integration methods were as described above for gross and net photosynthetic rates. While the oxygen-based methods described above measure the gross rate of organic carbon production by phytoplankton and the net rate of organic carbon production by the microplankton community, ^{14}C uptake measures the photosynthetic production of POC that is not respired or released as DOC on time scales $<$24 h.

Nitrate uptake. We measured rates of nitrate uptake, and estimated rates of nitrate-based new production (Eppley and Peterson, 1979), from conversion of ^{15}N-labeled nitrate ($^{15}NO_3^-$) to organic matter retained by glass-fiber filters (GFF; nominal pore size $\sim$0.7 μm) similar to those used for ^{14}C measurements of POC production rates (Sambrotto and Mace, 2000). Sampling depths, incubation conditions and vertical integration methods were as described above for ^{18}O and ^{14}C incubations, except that no correction for photoinhibition was found to be necessary for the ^{15}N measurements. Those incubations in a separate set of incubators were not subject to the same over-collection of light as those used for the ^{14}C and oxygen studies. We converted the measured

rates of nitrate uptake to carbon-based estimates of new production using the Redfield C:N mole ratio of 6.6 (Redfield et al., 1963).

Biogenic silica production. We measured rates of $BSiO_2$ production from the conversion of ^{32}Si-labeled silicic acid ($^{32}Si(OH)_4$) to particulate matter retained by polycarbonate membrane filters (Poretics, Inc.) with a pore diameter of 0.4 μm (Brzezinski et al., 2001). Sampling depths, incubation conditions and vertical integration methods were as described above for ^{15}N incubation experiments, but we included a sample from the depth of 0.1% surface irradiance in all profiles. That deeper sample was added because data from other areas have often shown that $BSiO_2$ production extends to greater depths than does either photosynthesis or nitrate uptake (e.g. Nelson and Brzezinski, 1997). This was true also in the AESOPS study (Brzezinski et al., 2001).

Seasonal net production of organic carbon and biogenic silica. We estimated these from the observed seasonal drawdown of NO_3^- and $Si(OH)_4$ in surface waters. Nutrient conditions in the study area at the beginning of the first *Revelle* cruise in October 1997 indicate that little biological removal had occurred since the time of deep convective mixing the previous winter (e.g., Morrison et al., 2001). Nutrient concentrations subsequently diminished as a result of biological uptake, with the greatest drawdown occurring north of 66°S (Morrison et al., 2001; Brzezinski et al., 2001). We obtained minimum estimates of the seasonal net production of POC and $BSiO_2$ from the vertically integrated depletion of NO_3^- and $Si(OH)_4$ in the upper 50–100 m. We estimated net $BSiO_2$ production directly from $Si(OH)_4$ drawdown (Sigmon et al., 2002) and POC production from NO_3^- drawdown multiplied by the Redfield ratio of 6.6 (Tables 1 and 3).

POC and $BSiO_2$ export from the upper 100 m. We estimated POC and $BSiO_2$ export from measurements of ^{234}Th, a naturally occurring particle-reactive radionuclide produced from a long-lived soluble precursor, ^{238}U (Buesseler, 1998 and references therein). We measured ^{234}Th activity profiles (generally 5 depths between the surface and 100 m) during the four *Revelle* cruises between October 1997 and March 1998. By measuring the ^{234}Th deficit, calculated as the vertically integrated difference between the ^{234}Th activity and that of its parent ^{238}U (^{238}U activity can be estimated from salinity), we calculated the export flux of ^{234}Th on sinking particles. We used these data and the measured ratios of particulate ^{234}Th to the POC and $BSiO_2$ retained on 70-μm screens to estimate POC and $BSiO_2$ fluxes at 100 m (Buesseler et al., 2001). We obtained independent estimates of $BSiO_2$ export from the upper 50 m based on seasonal changes in the total Si inventory (vertically integrated $[Si(OH)_4]$ + vertically integrated $BSiO_2$; Sigmon et al., 2002). No parallel estimate of POC export from the upper 50 m was made because we do not have adequate information on changes in the dissolved organic carbon (DOC) inventory in surface waters.

POC and opal fluxes to 1000 m. The fluxes of POC and $BSiO_2$ to 1000 m were calculated directly from material collected by sediment traps at four sites within the study area (Honjo et al., 2000). There is increasing evidence that the trapping efficiency of moored traps deployed in the mesopelagic zone can be $<100\%$ (Yu et al., 2001; Scholten et al., 2001). The thorium- and protactinium-based efficiency estimates employed by those authors are complicated in the Southern Ocean by the presence of a large advective supply of nuclides via upwelling of deep waters. Nevertheless, the 1000 m AESOPS traps collected a flux of ^{230}Th ranging from 46% to 90% of its rate of production by ^{234}U decay in the overlying water column (Chase, 2001). This suggests trapping efficiencies for the AESOPS traps were between 50% and 100%. Because of the uncertainty in estimating advective fluxes of nuclides on a site-specific basis, and because the $<100\%$ efficiencies identified by deficits in scavenged isotopes may be hydrodynamic and involve particle sorting in some unknown, composition-dependent manner, we have not corrected trap fluxes for possible undertrapping. The reported particle flux estimates to 1000 m thus represent minimum values, with maximum values being about twice the reported values.

Benthic remineralization of organic carbon and biogenic silica. We calculated rates of biogenic silica dissolution in the seabed from the efflux of

Table 3
Estimated annual fluxes of organic carbon and biogenic silica in the Southern Ocean at 170°W

Depth	Process	Method	Northern ACC (55°–59 °S)	Polar Frontal Region (59°–61.5 °S)	Southern ACC (61.5°–65.5 °S)	Rose Gyre (61.5°–68.5 °S)
A. Organic carbon fluxes (mol C $m^{-2} y^{-1}$)						
Euphotic zone	Gross photosynthesis	^{18}O conversion from H_2O to O_2	16	12	15	—[2]
Euphotic zone	Net community production	$d[O_2]/dt$	1.6	3.2	6.6	—[2]
Euphotic zone	POC production	^{14}C uptake	6.9	8.5	8.7	3.7
Euphotic zone	New production	$^{15}NO_3^-$ uptake	2.6	3.9	3.8	—[2]
50 m	New production	Seasonal NO_3^- drawdown	2.1	2.6	3.2	1.7
100 m	Particulate export	^{234}Th deficit, > 70 μm POC	2.5	2.3	2.7	1.7
1,000 m	Particulate flux	Sediment trap collections	0.17	0.17	0.21	0.14
Seabed	Particulate rain	Remineralization + burial[1]	0.071 – 0.074	0.055 – 0.063	0.15 – 0.21	0.088–0.14
Seabed	Remineralization	Pore-water NO_3^- profiles	0.070	0.061	0.20	0.14
Seabed	Remineralization	Pore-water TCO_2 & alkalinity profiles	0.073	0.053	0.14	0.087
Seabed	Long-term burial	^{230}Th-normalized accumulation	0.0012	0.0017	0.0062	0.0014
B. Biogenic silica fluxes (mol Si $m^{-2} y^{-1}$)						
Euphotic zone	Gross production	^{32}Si uptake	0.76	1.9	3.0	1.3
Euphotic zone	Net production	Seasonal $Si(OH)_4$ drawdown	0.35	0.95	2.4	0.69
50 m	Export	Seasonal ($Si(OH)_4 + BSiO_2$) drawdown	0.32	0.88	2.2	0.51
100 m	Particulate export	^{234}Th deficit, > 70 μm $BSiO_2$	0.64	1.4	1.4	0.34
1,000 m	Particulate flux	Sediment trap collections	0.28	0.38	0.94	0.21
Seabed	Particulate rain	Remineralization plus burial	0.29	0.34	1.4	0.26
Seabed	Remineralization	Pore-water $Si(OH)_4$ profiles	0.27	0.29	1.2	0.24
Seabed	Long-term burial	^{230}Th-normalized accumulation	0.016	0.048	0.16	0.016

[1] Range in POC rain represents that resulting from the two independent estimates of remineralization

[2] $H_2^{18}O$, $d[O_2]/dt$ and $^{15}NO_3^-$ incubation data in the Ross Gyre are insufficient to provide direct estimates of annual gross photosynthesis, net community production or new production.

$Si(OH)_4$ from the sediment at the seven benthic stations. We estimated rates of organic carbon remineralization at those same stations by two independent methods, one based on effluxes of alkalinity and total CO_2 (TCO_2), and the other from efflux of NO_3^-. Effluxes were estimated as described by Sayles et al. (2001) from the measured vertical profiles of pore-water solutes in the upper 20 cm of the sediment, determined using in situ pore-water sampling instruments exclusively for alkalinity and TCO_2 and combining in situ and shipboard methods for $Si(OH)_4$ and NO_3^-. Efflux estimates were based on the assumption that all flux is diffusive and proceeds in accordance with Fick's first law.

Long-term burial of organic carbon and biogenic silica. We calculated organic carbon and opal accumulation rates from measurements of opal, organic carbon and ^{230}Th in the top 4 cm of multicores collected at the seven benthic stations. The ^{230}Th method for obtaining vertical flux assumes that the flux of ^{230}Th to the sea floor is constant and equal to its production from ^{234}U decay in the overlying water column. Following François et al. (1990) and Suman and Bacon (1989), we derived the burial flux of organic carbon and biogenic silica (F_S, in $g\,cm^{-2}\,yr^{-1}$) by normalizing to the known constant flux of ^{230}Th:

$$F_S = (C_S/A_{Th}) \times P_{Th}, \quad (3)$$

where C_S is the weight-fraction of the component of interest, A_{Th} is the activity of ^{230}Th in the sediment, and P_{Th} is the ^{230}Th production rate, a function of the depth of water overlying the coring site (Sayles et al., 2001).

Rain of POC and opal to the sea floor. For both POC and $BSiO_2$, we estimated delivery to the sea floor as the sum of benthic remineralization plus long-term burial.

2.3. Sub-regions for constructing vertical budgets

Any attempt to construct a vertical elemental budget based on measured fluxes hinges on the assumption that changes in flux with depth result mainly from the production and recycling processes operating in that region. Lateral injection of material produced where production rates are either significantly higher or significantly lower would cause the apparent vertical budget to be aliased by lateral effects. The entire area under consideration in this study is dominated by the eastward-flowing ACC, with zonal transport extending from the surface to the bottom (Gordon and Molinelli, 1986). The Southern Ocean has been characterized biogeochemically as a series of zonal bands, in which properties change much more rapidly in the meridional direction than in the zonal direction (Tréguer and Jacques, 1992; Banse, 1996; Moore et al., 2000). We have thus divided the AESOPS study area into four hydrographically and ecologically distinct sub-regions, arranged spatially as zonal bands. We constructed vertical budgets for organic carbon and biogenic silica in each band, using fluxes measured in the water column and upper seabed. The four bands represent the following sub-regions:

1. The northern ACC (55°–59°S). This zone is situated entirely north of the APF. It is characterized by high surface nitrate and phosphate concentrations (>15 and $>2\,\mu M$, respectively), but relatively low silicic acid concentrations ($\sim 10\,\mu M$) prior to the onset of phytoplankton growth in spring (Morrison et al., 2001). This sub-region lies within an ecological zone that Banse (1996) referred to as the "subantarctic water ring", where there is relatively little seasonal change in chlorophyll.
2. The polar frontal region (59°–61.5°S). This is the zone in which the maximum meridional gradients in both surface and subsurface temperature and density are located at all times of year (Moore et al., 1999) and the site of the main meridional gradient in surface-layer [$Si(OH)_4$] in early spring (Morrison et al., 2001). It is also the zone of maximum mean eastward velocity of the ACC and maximum in mesoscale variability and eddy energy (Barth et al., 2001). This zone has been reported to be the site of intense phytoplankton blooms in the Atlantic sector of the ACC during spring and summer (e.g., Laubischer et al., 1993; Bathmann et al., 1997).
3. The southern ACC (61.5°–65.5°S). This zone lies entirely within the ACC, south of the APF.

In the vicinity of 170°W the southern ACC is almost completely ice-covered in late winter and is entirely ice-free by late summer. It has high surface $[Si(OH)_4]$ (35–55 μM) in late winter (Morrison et al., 2001), and is the zone within which we observed the main biological event in surface waters during the spring and summer of 1997–1998: A diatom bloom developed between the southern edge of the APF and the winter ice edge in early December, and then propagated southward across the southern ACC between December and early February, depleting surface $[Si(OH)_4]$ to $<2\,\mu M$, and occasionally to $<1\,\mu M$, to at least as far south as 65°S (Brzezinski et al., 2001).

4. The Ross Gyre (65.5°–68°S). This zone lies south of the SACCF, and surface waters passing through 170°W at these latitudes come mainly from the Ross Sea shelf (e.g. Gordon and Molinelli, 1986). This zone is ice-covered for all but ~100 days each year, and is south of the area from which there is evidence of a diatom bloom during either 1996–1997 or 1997–1998 (Honjo et al., 2000; Brzezinski et al., 2001).

Each of these zones included one sediment-trap mooring site, one to three stations at which benthic fluxes were measured, and 4–24 stations at which surface-layer rate data were obtained during AESOPS. The latitude and bottom depth of each mooring site and benthic site and the time interval during which surface-layer rate measurements were made within each of these zones are shown in Table 2.

2.4. Estimation of annual POC and $BSiO_2$ fluxes

The available rate data are most readily compared when they are expressed as estimated annual fluxes, in mol C or Si $m^{-2}\,yr^{-1}$. Of the data sets obtained, only the 1000-m sediment-trap data permit an annual flux per m^{-2} to be calculated directly (Honjo et al., 2000). Our other rate measurements integrate over shorter or longer time scales: 1 day for photosynthesis and nutrient uptake in surface waters (Sambrotto and Mace, 2000; Brzezinski et al., 2001; Dickson and Orchardo, 2001), several weeks for seasonal nutrient drawdown and ^{234}Th-based export (Buesseler et al., 2001; Sigmon et al., 2002), several months to several years for benthic remineralization, and more than 1000 years for burial (Sayles et al., 2001). We have thus either extrapolated or interpolated those rate data as described below to estimate annual fluxes.

Primary production, new production biogenic silica production and export of C and Si. We obtained vertical profiles of C, NO_3^- and $Si(OH)_4$ uptake rates between the sea surface and the base of the euphotic zone (1% of surface irradiance for photosynthesis and NO_3^- uptake, 0.1% of surface irradiance for $Si(OH)_4$ uptake). The measured rates were generally very low at the greatest depth sampled (Dickson and Orchardo, 2001; Brzezinski et al., 2001). We thus obtained reasonably direct measurements of the vertically integrated daily rate of each process, (in mmol C, N or Si $m^{-2}\,d^{-1}$) at the location sampled on the date when the experiment was performed. Within each sub-region our data set consists of 4–24 daily measurements of vertically integrated photosynthesis or nutrient uptake, taken over some known period of time in spring and summer (Table 2). Those periods ranged from 9 to 134 days, with all in the three most northerly sub-regions being $\geqslant 72$ days. All data records from the Ross Gyre were $\leqslant 50$ days long because ice cover prevented the ship from operating there until mid January.

We estimated export of POC and opal from the upper 100 m based on ^{234}Th deficits in the upper 100 m, which included the full depth range over which such deficits were measurable (Buesseler et al., 2001). We therefore obtained reasonably direct estimates of POC and opal export, averaged over the several-weeks time scale on which ^{234}Th deficits integrate (e.g. Buesseler et al., 1992). We collected ^{234}Th data over time intervals similar to those for photosynthesis and nutrient uptake data (113–134 days in the ACC, 41 days in the Ross Gyre).

We used several different methods to estimate the time-integrated productivity, nutrient uptake, and export during the period covered by the data. Temporal integration methods differed because of

differences in the temporal coverage. We measured rates of $BSiO_2$ production, POC export from the upper 100 m and $BSiO_2$ export from the upper 100 m during all four cruises, and calculated the time-integrated rates of those processes within each sub-region by trapezoidal integration of the time-course data within the appropriate latitude band. We measured rates of gross photosynthesis, POC production, new production and net community production on only the December/January and February/March cruises. That sampling strategy missed little biological activity during the October/November cruise, which was conducted before spring stratification and the onset of net nutrient drawdown (Morrison et al., 2001). However, it produced a $\sim$40-day gap (early January through mid February), which coincided with the peak of the summer diatom bloom in the southern ACC (e.g. Brzezinski et al., 2001). We integrated through that part of the growing season based on empirical relationships between measured rates and other properties that were measured on all cruises.

Vertically integrated photosynthetic rates were strongly correlated with surface irradiance in December, early January and late February/March (R. Barber and J. Marra, unpublished data). We therefore used measured surface irradiance and the observed relationship between irradiance and productivity to estimate POC production between early January and mid February, when no direct measurements were made. It was not necessary to correct surface irradiance data for ice cover in the three sub-regions located within the ACC because the entire ACC was ice-free by late December (Smith et al., 2000). Primary productivity in the Ross Gyre was measured only during late February and early March (Table 2), and the measured rates were extrapolated to the 100-day ice-free period in that sub-region.

We estimated new production during January and early February based on the observed ratio of vertically integrated $^{15}NO_3^-$ uptake to surface chlorophyll during December, late February and early March. That ratio was nearly constant at $\sim 5\,\mathrm{mmol\ N\,m^{-2}\,d^{-1}}$ (μg Chl $a\,\mathrm{l^{-1}})^{-1}$ until late in the season when it decreased somewhat (Sambrotto and Mace, 2000). We used that relationship, along with surface chlorophyll estimated from NASA's SeaWiFS sensor, to estimate new production in each sub-region during the temporal gap in the ^{15}N data record. No estimate of annual gross photosynthesis, net community production or ^{15}N-based estimate of annual new production in the Ross Gyre is possible, because of the small number of ^{18}O and ^{15}N incubation experiments performed there.

The time-integrated production and export in spring and summer are lower than the corresponding annual fluxes because they do not account for the rest of the year. However, our data record clearly included the period of maximum phytoplankton productivity and export (e.g., Brzezinski et al., 2001; Buesseler et al., 2001). Therefore, we estimated the annual flux estimates by a uniform extrapolation method that draws upon the one genuinely year-round data record we have in each sub-region, the particle fluxes collected by sediment traps at $\sim$1000 m (Honjo et al., 2000).

The sediment-trap data from all AESOPS sites show that the fluxes of both POC and $BSiO_2$ to 1000 m were greatest in summer, with a long period of much lower flux through the autumn, winter and early spring (Honjo et al., 2000). All upper-ocean production and export measurements were made in the spring and summer (Table 2). We therefore estimated annual production and export based on the assumption that our sampling period included the annual production and export maxima for both POC and $BSiO_2$. Mathematically, we assumed that the time period included in our data record (T_D) was the most productive period of that length during the year. We then identified the period of comparable length in the sediment-trap record (T_F) that had the highest integrated POC or $BSiO_2$ flux to 1000 m at the mooring site located in the same sub-region (Honjo et al., 2000). For example, our record on $BSiO_2$ production rates in the polar frontal region (59°–61.5°S) covers 132 days, from November 2 1997 through March 13 1998 (Table 2). The period of similar length that yields the highest mean $BSiO_2$ flux to 1000 m at the mooring site within that sub-region (60.27°S) was a 134-day period from November 30 1996 through April 13 1997. (The data records consistently show a seasonal lag between the period of maximum

production in surface waters and that of maximum particle flux to 1000 m.) We then calculated the annual production or export (P_A) in mol C or Si m^{-2} yr^{-1} as

$$P_A = P_D \frac{T_F F_A}{T_D F_D}, \quad (4)$$

where P_D is the time-integrated production or export during the period covered by data (mol C or Si m^{-2}); F_A is annual flux to 1000 m (mol C or Si m^{-2} yr^{-1}); F_D is flux to 1000 m during the highest-flux period of a length similar to that of the data record on production (mol C or Si m^{-2})

This estimation method assumes that the shape of the seasonal time course of upper-ocean productivity and particle export parallels that of the seasonal time course of particle flux to 1000 m, but it is unaffected by the time lag between production in surface waters and arrival at 1000 m. The upper-ocean rate estimates derived in this way are conservative, as we cannot be certain that (in the example given above) the 132-day period covered by our data is the single most productive 132-day period that could have been chosen during the year. But this scheme provides a far more realistic estimate than could be obtained either by ignoring production and export during autumn and winter or by extrapolating spring and summer rates to the entire year.

Net production of $BSiO_2$ and POC and export of $BSiO_2$ based on nutrient drawdown and changes in $BSiO_2$ with time. Nutrient drawdown calculations are useful only for spring and summer, when surface-layer nutrient concentrations decreased with time. They provide minimum estimates of annual net production because they contain no information for the autumn and winter when rates of nutrient resupply by upwelling and mixing exceed those of nutrient uptake by phytoplankton. Even the spring/summer estimate is conservative, because it is based on the excess of net nutrient use in surface waters over resupply by upwelling and mixing (e.g., Jennings et al., 1984). There are no reliable criteria for evaluating the uncertainty in estimates of this kind; they provide a hard minimum, but no information on the maximum. The resulting minimum estimates of net $BSiO_2$ and POC production are reported primarily for comparison with others, which can be extrapolated to consider potentially significant rates in autumn and winter (e.g., annual new production based on $^{15}NO_3^-$ uptake or export based on ^{234}Th deficits).

Benthic remineralization and burial of POC and opal. Benthic remineralization estimates are based on measurements made at a single time point for each region (March–April 1998). In calculating annually averaged fluxes, we considered the possible effects of temporal variability on fluxes (Sayles et al., 2001). The estimated temporal variability was small at the southernmost site (66.14°S), with maximum fluxes estimated to be 25% greater than the annual mean. This difference is similar to the spatial variability found in the Ross Gyre region. The potential temporal variability is most significant at 63.17°S, where a fluff layer was observed just above the sediment surface and the maximum flux was estimated to be 1.6–2.3 times the annual mean (Sayles et al., 2001). If this site is representative of all those at which a fluff layer was present (61.88°S, 63.17°S and 64.20°S), then a correction would have to be applied to fluxes calculated from high-resolution pore-water data at each of these sites. The corrected fluxes, calculated from high-resolution pore-water profiles of NO_3^-, are higher than fluxes calculated from lower resolution alkalinity and TCO_2 profiles by about 40%. This difference is similar to the spatial variability that was averaged to give the regional flux estimate for the southern ACC region in Table 3. Modeling indicates that no seasonal variability in POC remineralization was likely at sites within and north of the polar frontal region (Sayles et al., 2001). The NO_3^--based fluxes shown in Table 3 have been corrected for the model-derived effect of seasonal variability. The fluxes calculated from alkalinity and TCO_2 data, which are based on profiles with coarser depth resolution below the sediment–water interface, do not include the correction.

The corrected NO_3^--based fluxes are about 40% higher than those calculated from alkalinity and TCO_2. This difference is similar to the spatial variability that was averaged to give the regional

flux estimates for the southern ACC in Table 3. Thus the range of estimates for the Ross Gyre and southern ACC may reflect both spatial variability and the difference between two independent methods of calculation. Additional modeling demonstrated that the time scale of opal remineralization in sediments throughout the region is long enough that no seasonal variability in benthic dissolution rates is likely for opal. The regional average benthic remineralization values reported for the northern ACC have large uncertainty ($\pm 80\%$ for POC and $\pm 50\%$ for opal) because they combine data from two sites (58.69°S, water depth 4345 m, and 56.88°S, 4969 m) with very different benthic fluxes (Sayles et al., 2001).

2.5. Uncertainty in the estimated annual fluxes

As noted above, some of our individual flux estimates are subject to quantifiable uncertainty of up to a factor of two. In addition, while rates of biological processes in surface waters are inherently measured to within $\pm 5\%$ by isotopic tracer methods, vertical integration and seasonal extrapolation of those rates introduce additional errors, which cannot be quantified well by analytical or statistical criteria. Burial fluxes estimated by ^{230}Th-normalization have an uncertainty of up to $\pm 30\%$ associated with the assumption that the flux of ^{230}Th is equal to its production rate (Henderson et al., 1999). Further uncertainty is introduced by the fact that the various rate measurements integrate over time scales ranging from 1 day to >1000 years, and that the surface-layer and 1000 m data were obtained during different years. Fluxes of POC and opal to 1000 m were measured mostly during 1996–1997, while upper-ocean fluxes were measured only during the spring and summer of 1997–1998. The cumulative effect of these uncertainties is that small differences between estimated fluxes should not be interpreted as having any significance. While there is no reliable way to evaluate the uncertainty associated with the estimated annual fluxes, we believe that estimates for the same phase (i.e. opal or POC) are distinguishable from one another only if they differ by at least a factor of two.

3. Results and discussion

All estimated annual fluxes of POC and $BSiO_2$ in the Pacific sector of the Southern Ocean between November 1996 and March 1998 are presented in Table 3. Estimates are reported to two significant figures for consistency but, as noted above, small (<2-fold) differences between flux estimates should not be interpreted as having significance. Many of the estimated differences are much greater than a factor of two, however, and they show several major features of the C and Si cycles in the region:

3.1. Relationships among gross photosynthesis, net community production and POC production

The estimated annual gross photosynthesis, net community production and POC production in the three sub-regions located within the ACC are presented in Fig. 2. Data records for gross photosynthesis and net community production obtained in the Ross Gyre are not long enough to permit estimates of annual production. Estimated annual POC production based on ^{14}C uptake ranged from 6.9 to 8.7 mol C m^{-2} yr^{-1}. Estimated gross photosynthesis ranged from 12 to 16 mol C m^{-2} yr^{-1}, 1.4–2.3 times annual POC production, in those sub-regions. Like POC production, gross photosynthetic rates were fairly uniform across the ACC (Fig. 2). Estimated net community production increased southward from 1.6 mol C m^{-2} yr^{-1} in the northern ACC to 6.6 mol C m^{-2} yr^{-1} in the southern ACC. The ratio of net community production to gross photosynthesis increased southward, from 0.10 in the northern ACC, to 0.27 in the polar frontal region and 0.43 in the southern ACC. That ratio estimates the fraction of photosynthetically produced organic matter that is available for export from the euphotic zone, with high ratios indicating efficient export and low ratios intense near-surface recycling. The data thus suggest that 57–90% of gross photosynthetic production was remineralized within the euphotic zone across the entire region, with intensity of recycling diminishing to the south.

The difference between the estimates of annual gross photosynthesis and annual POC production

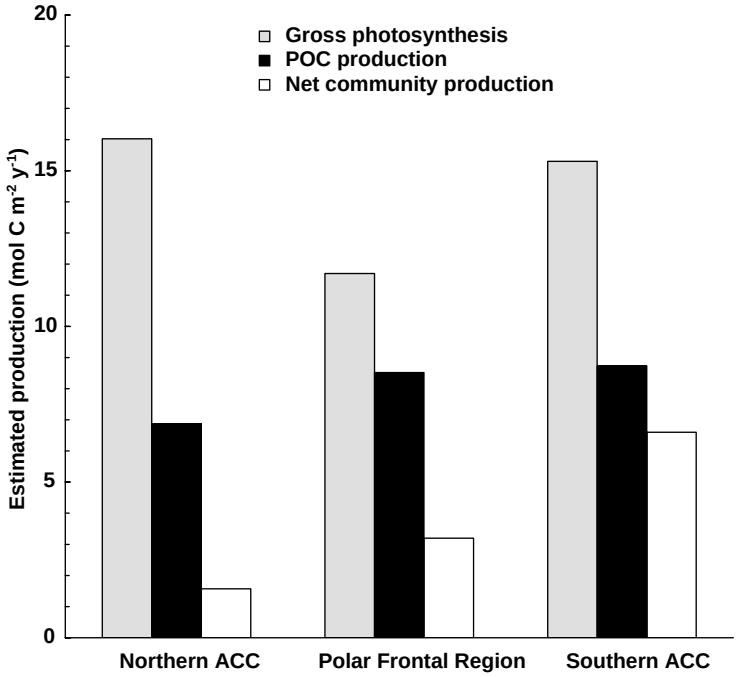

Fig. 2. Estimated annual gross photosynthesis (from rates of transformation of ^{18}O from H_2O to O_2) POC production (from rates of ^{14}C conversion from HCO_3^- to POC) and net community production (from net rates of change in dissolved $[O_2]$) estimated from incubation data in each of the three sub-regions of the ACC selected for constructing vertical POC budgets: the northern ACC (55°–59°S), polar frontal region (59°–61.5°S) and southern ACC (61.5°–65.5°S). Data records for gross photosynthesis and net community production obtained in the Ross Gyre (65.5°–68°S) were not long enough to permit estimates of annual production.

is not an artifact arising from the temporal extrapolation methods, as it is apparent in the original station data. Moreover, gross photosynthetic rates estimated by the difference between $d[O_2]/dt$ measured in light and dark bottles averaged 92% of the gross production rate measured with ^{18}O during the spring cruise, providing support for the isotopic measurements (Dickson and Orchardo, 2001). Differences between gross photosynthesis and POC production can arise from a variety of autotrophic metabolic processes and from heterotrophic respiration (Bender et al., 1999; Laws et al., 2000). The data imply that 30–60% of the carbon fixed photosynthetically by phytoplankton was respired back to inorganic C and/or released as DOC within 24 h. On an annual basis, net community production was $<50\%$ of gross photosynthesis in every sub-region, and reasonably close to POC production only in the southern ACC. The apparent differences between annual net community production and annual POC production are due to net heterotrophic conditions that existed over much of the region in the late summer (Dickson and Orchardo, 2001). Unlike net O_2 production rates, ^{14}C uptake rates can never be negative. These relationships suggest that respiration and release of DOC in surface waters combine to make annual POC production significantly lower than annual gross photosynthesis in the Pacific sector of the ACC.

Export of organic carbon from surface waters is dominated by the downward transport of POC, and several of our data sets (e.g. ^{234}Th removal from the upper 100 m and particle fluxes to sediment traps at 1000 m) specifically measure the POC flux. We will therefore use POC production, as measured by ^{14}C uptake, as the main surface source term in the organic carbon budget. Using gross photosynthesis would increase that

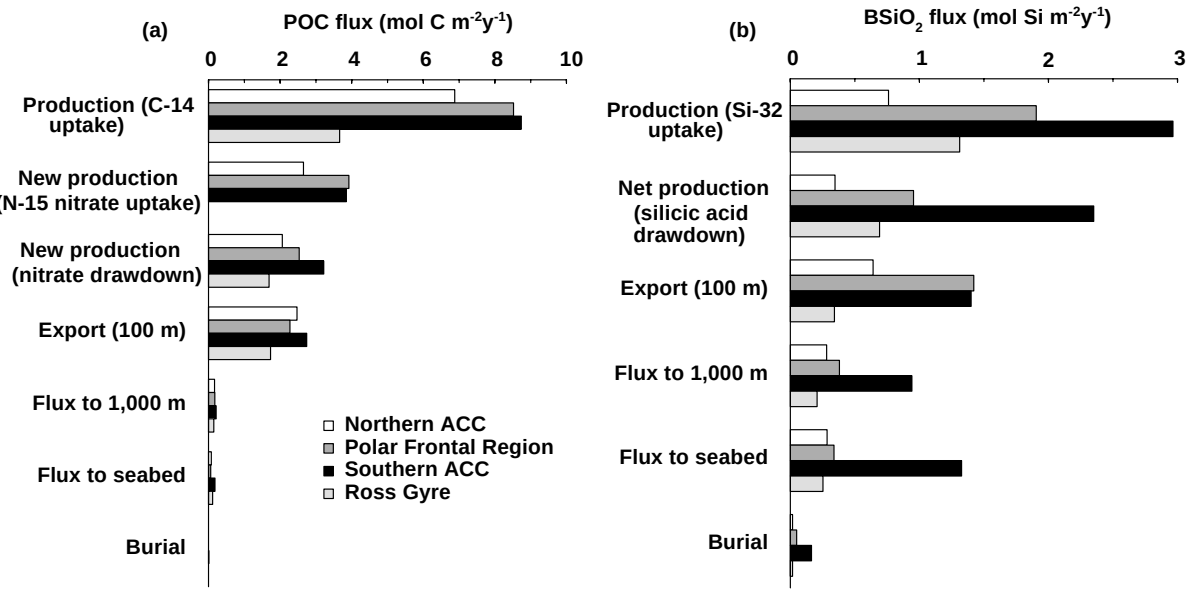

Fig. 3. Estimated annual fluxes of POC (A) and $BSiO_2$ (B) in each of the four sub-regions. See text for descriptions of the data sets and estimation methods used. The estimated POC flux to the seabed represents the sum of burial plus the mean of the two independent estimates of benthic remineralization shown in Table 3.

surface source term by ~40% in the polar frontal region, and by 75–130% in the southern and northern ACC (Fig. 2). The estimated fraction of surface-produced organic matter exported from surface waters, reaching 1000 m or delivered to the seabed in the northern and southern ACC would thus decrease by approximately a factor of two if we considered gross photosynthesis as the surface source term.

3.2. Vertical budget for particulate organic carbon

The estimated annual fluxes of POC in each of the four sub-regions are shown in Fig. 3a. It is clear from these estimates that the annual downward flux of POC diminishes dramatically with depth. Several other features of the carbon cycle in this sector of the Southern Ocean are apparent from this budget.

Primary productivity. The annual production of POC in surface waters was 6.9–8.7 mol C m^{-2} yr^{-1} (~80–105 g C m^{-2} yr^{-1}) in each sub-region except the Ross Gyre, where it was ~3.7 mol C m^{-2} yr^{-1} (~45 g C m^{-2} yr^{-1}). The lower annual productivity in the Ross Gyre resulted from the combined effects of a shorter ice-free season and the fact that no significant phytoplankton bloom developed there during the ice-free period. The estimated POC production throughout the AESOPS study area between 55°S and 65.5° S is somewhat higher than most other estimates of annual primary productivity in the Southern Ocean south of 55°S, which are generally <50 g C m^{-2} yr^{-1} (Antoine et al., 1996, Behrenfeld and Falkowski, 1997).

New production and POC export from the upper 100 m. The AESOPS data permit three independent estimates of new production or POC export. These are:

1. annual new production estimated from ^{15}N tracer measurements of nitrate uptake,
2. seasonal new production in spring and summer estimated from the observed drawdown of nitrate in surface waters, and
3. annual POC export from the upper 100 m estimated from ^{234}Th deficits in surface waters and the POC content of the >70 μm particles

assumed to be responsible for most ^{234}Th export.

Fig. 3a shows that these three estimates of new or export production are in excellent agreement, and that all indicate this export term to be ~30–40% of annual POC production throughout this sector of the ACC. No ^{15}N-based estimate of new production can be made for the Ross Gyre, but the new-production estimate based on nitrate drawdown agrees closely with the export estimate based on ^{234}Th in that system as well. Both suggest that ~50% of the POC produced annually is exported. There is considerable—and difficult to quantify—uncertainty associated with each of these estimates, but they are based on completely different data sets and thus genuinely independent. One feature of the individual data sets not apparent in the annual estimates is that there was a significant temporal offset between new production and POC export. During December 1997, when the main diatom bloom was developing and propagating southward (Brzezinski et al., 2001), vertically integrated new production calculated from measured rates of $^{15}NO_3^-$ uptake greatly exceeded POC export from the upper 100 m calculated from ^{234}Th deficits and POC content of large particles (Sambrotto and Mace, 2000; Buesseler et al., 2001). By February, when no phytoplankton bloom was observed in the study area and there were extensive areas of net heterotrophy in surface waters (Brzezinski et al., 2001; Dickson and Orchardo, 2001), ^{234}Th-based measurements of POC export significantly exceeded $^{15}NO_3^-$-based measurements of new production (Sambrotto and Mace, 2000; Buesseler et al., 2001). This temporal offset is similar to that observed between the start of elevated new production during the southwest monsoon in the Arabian Sea and the initial increase in ^{234}Th deficits (Buesseler et al., 1998; Sambrotto, 2001). The offset may represent the accumulation of biomass in surface waters between the initial establishment of favorable growth conditions and the increase in sinking and grazing losses.

Data from AESOPS thus provide robust evidence that new production and POC export were 1.7–3.8 mol C m^{-2} yr^{-1} throughout the ACC at 170°W during 1997–1998. These estimates are in the same general range as new-production estimates based on seasonal nitrate drawdown the Indian Ocean sector of the ACC, which range regionally from 0.9 to 3.5 mol C m^{-2} yr^{-1} (Pondaven et al., 2000). They are somewhat lower than the mean new production of 5.1 mol C m^{-2} yr^{-1} over the Ross Sea shelf estimated from $^{15}NO_3^-$ uptake rates (Nelson et al., 1996). Our three independent estimates of new production and POC export in the AESOPS study area are also in the general range predicted by the recent biogeochemical model of Schlitzer (2000), which estimates POC export from ocean circulation patterns and the distributions of dissolved oxygen, nutrients and TCO_2. Those model results predict export fluxes of 2–6 mol C m^{-2} yr^{-1} throughout the Pacific sector of the Southern Ocean (see Schlitzer's Fig. 9). Our results are also in general agreement with recent estimates of new production based on seasonal drawdown of HPO_4^{2-} (Louanchi and Najjar, 2000), which suggest a mean new production of 2–2.5 mol C m^{-2} yr^{-1} throughout the Southern Ocean south of 40°S. The Pacific sector at 170°W thus seems to be quite typical of the Southern Ocean with respect to annual POC export.

In each sub-region of the ACC new production estimated from the $^{15}NO_3$ uptake measurements somewhat exceeds POC export fluxes based on ^{234}Th deficits (Fig. 3a). None of these differences reaches the factor-of-two level that is necessary to accept a difference in fluxes as genuine. However, sediment-trap collections indicate that some of the discrepancy may be attributed to the nitrogen-rich nature of the sinking material in this region, particularly at the end of the growing season (Honjo et al., 2000).

Our data provide no evidence that annual gross photosynthesis, POC production, net community production or POC export is higher in the polar frontal region than in the waters to the north or south (Figs. 2 and 3a). The data also provide no indication that annual production or export of $BSiO_2$ is higher in the polar frontal region than in the rest of the ACC at 170°W (Fig. 3b). Upwelling associated with mesoscale meanders in the APF

has been shown to be a potential source of both macro- and micronutrients to the surface layer in this sector (Barth et al., 2001), and the APF is the site of intensified primary productivity in other sectors of the ACC (e.g. Laubischer et al., 1993; Bathmann et al., 1997). However, production and export rates measured at 170°W suggest that any stimulation of either process by enhanced nutrient supply within the APF is negligible on an annual basis.

Transport of POC to the deep ocean and the seabed. The flux of POC to 1000 m ranged from ~140 to ~210 mmol C m^{-2} yr^{-1} (Table 3, Fig. 3a). Those fluxes, which were calculated directly from year-round sediment-trap collections (Honjo et al., 2000), contain less uncertainty than do estimates extrapolated from spring and summer data. POC fluxes to 1000 m are consistently between 6% and 8% of the ^{234}Th-based estimate of POC export from the upper 100 m. Even if the 1000-m fluxes are systematically underestimated by 20–40% due to under-collection of sinking POC (Yu et al., 2001; Scholten et al., 2001), the clear implication is that ~90% of the POC exported from the upper 100 m is remineralized at depths <1000 m. This is a common observation in the ocean (e.g. Lee et al., 1998), supported in other systems by data showing that both the settling flux of POC and respiratory consumption of O_2 decrease quasi-exponentially with depth between 100 and 500 m (Martin et al., 1987; Jenkins and Goldman, 1985).

Remineralization of sinking POC in the upper 1000 m has particular significance for the carbon cycle in the Southern Ocean. If we seek to evaluate the rate at which biological pumping extracts CO_2 from the atmosphere and delivers it to the deep ocean as POC, that carbon must be exported to at least the shallowest depth that will not be ventilated during the following winter. Carbon remineralized at shallower depths will be released back to the atmosphere at the time of ventilation, resulting in no net transport to depth. Winter ventilation depths in the ACC are generally 200–300 m, and can be as deep as 500 m (Gordon and Molinelli, 1986). Thus the annual extraction of carbon from the atmosphere by biological processes in the Southern Ocean may be seriously overestimated by quantities such as new production and export production, which are well defined only for the upper 100 m and do not account for relatively shallow (100–500 m) subsurface recycling. Respiration below the euphotic zone but within the ventilated layer also may reduce the amount of material exported to depth. Daily net community production rates determined from incubations were more than twice those estimated from mixed-layer oxygen saturation levels (Dickson and Orchardo, 2001). This difference was found in spring, when mixed-layer depths greatly exceeded the depth of the euphotic zone and it was attributed to respiration of material below the euphotic zone. Lack of reliable information on organic matter remineralization between 100 and 500 m thus appears to be a major gap in our present ability to characterize the carbon cycle of the Southern Ocean.

A relatively high fraction (30–85%) of the POC that does penetrate to 1000 m, apparently reaches the sea floor. The most efficient transport of POC from 1000 m to the sea floor appears to occur south of the APF, where POC rain to the sea floor is 55–85% (and hence indistinguishable from 100%) of the flux to 1000 m. In contrast, we estimate that 30–45% of the POC that reaches 1000 m reaches the sea floor in the polar frontal region and northern ACC (Table 3). Bottom depths at 170°W are considerably shallower in the southern ACC and Ross Gyre than they are in the polar frontal region and northern ACC (Fig. 1). Depths at the sites where we measured benthic fluxes in the two more southerly subregions were ~2750–3300 m, as opposed to ~3980–4970 m to the north (Table 2). Thus the more efficient transport of POC from 1000 m to the sea floor in the northern part of the study area may result from the simple fact that the vertical distance those particles must travel is less. In general, the ~90% loss of POC between 100 and 1000 m and relatively efficient transport from 1000 m to the sea floor imply that pelagic remineralization of organic matter is much less intense below 1000 m than at shallower depths.

Benthic remineralization and burial. Benthic flux studies during AESOPS indicate that 97–99% of the POC that reaches the sea floor is remineralized

in the upper sediment and diffuses back to the water column as dissolved inorganic carbon (Table 3; see also Sayles et al., 2001). As a consequence, organic carbon is buried at a rate of only 1.2–6.2 mmol $C\,m^{-2}\,yr^{-1}$ beneath the Pacific sector of the ACC (Table 3). This burial represents only 0.02–0.07% of annual POC production and 0.008–0.04% of gross photosynthesis in surface waters (Table 3).

3.3. Vertical budget for biogenic silica

The estimated annual fluxes of biogenic silica in each of the four sub-regions are shown in Fig. 3b. While these estimates show that the downward flux of opal diminishes with depth, comparison with POC fluxes (Fig. 3a) shows that $BSiO_2$ flux decreases much less with depth than does POC flux. Several other features of the silica cycle and its relationship with the carbon cycle in the Pacific sector of the Southern Ocean are apparent from this budget.

Biogenic silica production in surface waters. The zone of relatively high and meridionally constant annual POC production between 55°S and 65.5°S is characterized by pronounced southward increases in both gross silica production (as estimated from measured rates of ^{32}Si uptake) and net silica production (as estimated by seasonal drawdown of $Si(OH)_4$). Estimated gross production of biogenic silica was 0.76, 1.9 and 3.0 mol $Si\,m^{-2}\,yr^{-1}$ in the ACC north of, within and south of the polar frontal region, respectively (Table 3, Fig. 3b). Net silica production ranged from 0.35 mol $Si\,m^{-2}\,yr^{-1}$ (~45% of gross $BSiO_2$ production) in the northern ACC to 2.4 mol $Si\,m^{-2}\,yr^{-1}$ (~80% of gross $BSiO_2$ production) in the southern ACC where the main diatom bloom was observed (Table 3, Fig. 3b).

Within each sub-region the difference between estimated gross and net $BSiO_2$ production was generally smaller than the factor-of-two difference that is needed to provide an interpretable estimate of silica dissolution in surface waters. There is, however, an additional data set that tends to corroborate the observed difference. ^{29}Si tracer experiments showed that vertically integrated silica dissolution in surface waters averaged 20–30% of vertically integrated $BSiO_2$ production during the main diatom bloom and 60–70% of silica production during periods of low productivity before and after that bloom (Brzezinski et al., 2001). The spatial and temporal coverage of ^{29}Si silica dissolution rate measurements are not sufficient to permit annual estimates comparable to the others reported here. However, the approximate magnitude of the difference between gross and net silica production indicated by the direct measurements of silica dissolution rates agrees well with those inferred by comparing silicic acid drawdown to gross silica production (Table 3).

The main factor controlling the southward increase in both gross and net $BSiO_2$ production between 55°S and 65.5°S appears to be the standing stock of $Si(OH)_4$ in surface waters at the end of winter. Before the onset of net diatom growth in spring, surface-layer $[Si(OH)_4]$ was ~10 μM in the northern ACC (55°–59°S) and 35–55 μM in the southern ACC (61.5°–65.5°S), with a strong gradient of southward-increasing concentrations in the polar frontal region (59°–61.5°S) (Morrison et al., 2001). Surface-layer $[Si(OH)_4]$ was drawn down to $<2\,\mu M$, and occasionally to $<1\,\mu M$, everywhere north of 65°S and the low residual concentrations were strongly limiting to further uptake by diatoms (Nelson et al., 2001). On a seasonal basis, 70–80% of the initial standing stock of $Si(OH)_4$ in the upper 50 m within each 1° latitude interval between 58°S and 65°S was exported as biogenic silica, resulting in seasonally integrated opal export that ranged from ~0.4 mol $Si\,m^{-2}$ at 58°S to ~2.2 mol $Si\,m^{-2}$ at 64°S (Sigmon et al., 2002). Thus the $Si(OH)_4$ initially available in surface water was exported efficiently throughout the ACC at 170°W and both $BSiO_2$ production and $BSiO_2$ export increased from north to south because that initial standing stock was lowest in the subantarctic, intermediate in the gradient region around the APF and highest south of the APF.

Biogenic silica export from surface waters and flux to the deep ocean and sea floor. Opal fluxes decreased between 100 and 1000 m, but by much less than did POC fluxes (Fig. 3). $BSiO_2$ flux decreased by an estimated 73% between 100 and

1000 m in the polar frontal zone, and by 33–55% in the other three sub-regions (Table 3). Thus an estimated 27–67% of the $BSiO_2$, as opposed to 6–8% of the POC, exported annually from surface waters penetrates to 1000 m in this sector of the Southern Ocean. The percentages calculated above would be aliased by any significant difference between $BSiO_2$ export in 1996–1997 (when the 1000-m fluxes were measured) and 1997–1998 (when export from the upper 100 m was measured). However, the selective preservation of opal that is apparent in Fig. 3 cannot be an artifact resulting from interannual differences unless opal export was much higher in 1996–1997 than in 1997–1998. As discussed above, surface $[Si(OH)_4]$ was depleted to $<2\,\mu M$ everywhere between 55°S and 65°S during 1997–1998. This nearly complete removal of the available $Si(OH)_4$ in 1997–1998 makes it highly unlikely that opal export could have been significantly higher during the previous year.

Our estimates imply that a very high fraction of the $BSiO_2$ that reached 1000 m reached the sea floor. Estimates for the four sub-regions range from 89% to 145% (Table 3), none of which is distinguishable from 100% given the uncertainty inherent in such estimates. The carbon budget shows that there was also relatively little remineralization of POC in the water column below 1000 m. The efficient transport of both $BSiO_2$ and POC from 1000 m to the sea floor in all four sub-regions could have at least two contributing causes. It is possible that the particulate material —both organic and siliceous—produced in surface waters already has had its most reactive components remineralized (for POC) or dissolved (for $BSiO_2$) by the time it reaches 1000 m. It is also possible that those particles that penetrate to 1000 m do so by sinking so rapidly that they cover the remaining distance to the sea floor in a very short time. Both processes may be significant; the sediment-trap records indicate a time lag on the order of 17 days between the maximum POC and opal fluxes to ~1000 m and the maximum fluxes to deeper traps at ~2900–4900 m (Honjo et al., 2000). That time lag is consistent with a bulk settling rate of $\sim 200\,m\,d^{-1}$.

Benthic dissolution and burial. The benthic flux data indicate that 83–95% of the $BSiO_2$ reaching the sea floor dissolves in the upper sediment (Sayles et al., 2001; see also Table 3). While this represents substantial recycling, it is considerably less intense than the 97–99% remineralization calculated above for the POC that reaches the sea floor. This differential recycling continues a process that appears to occur throughout the water column: POC is remineralized more rapidly than $BSiO_2$ within every depth interval, from surface water to the seabed. The cumulative effect is that the preservation efficiency (burial in the seabed/production in surface waters) is much greater for $BSiO_2$ than for POC. Estimated preservation efficiencies for $BSiO_2$ range from 1.2% in the Ross Gyre to 5.5% in the southern ACC, while those for POC range only from 0.02% in the northern ACC to 0.08% in the southern ACC.

Although the preservation efficiency for $BSiO_2$ appears to be ~60 times greater than that for POC throughout the AESOPS study area, it is not unusually high in comparison with opal preservation efficiencies elsewhere in the ocean. The 1.2–5.5% range of opal preservation efficiency calculated for the AESOPS study area is indistinguishable from the global mean of 2.5–3% estimated by Tréguer et al. (1995). Thus the AESOPS results from the Pacific sector are consistent with those recently presented by Pondaven et al. (2000) from the Indian sector: Opal preservation efficiency is not enhanced in the Southern Ocean, and thus is not the reason why extensive diatom-rich sediments are forming beneath low-productivity surface waters.

A consistent spatial pattern in the silica cycle. The southern ACC between 61.5°S and 65.5°S represents a local maximum in almost every Si flux estimated in the upper ocean, the deep ocean or the seabed (Fig. 3b). The sole exception to that pattern is opal export from the upper 100 m, where the maximum is somewhat broader and includes both the polar frontal region and the southern ACC. It is important to note in this regard that the different estimates consider not only different data sets but also different time intervals. Estimates of gross and net $BSiO_2$ production in surface waters

and opal export from the upper 100 m are all derived from data obtained in the spring and summer of 1997–1998 (Brzezinski et al., 2001; Sigmon et al., 2002; Buesseler et al., 2001; see also Table 2). Opal fluxes to 1000 m were measured from November 1996 through January 1998 and the estimated annual fluxes are influenced most strongly by data from the spring and summer of 1996–1997 (Honjo et al., 2000). Benthic dissolution fluxes (the main term in the estimated flux to the seabed) integrate time periods ranging from several months to several years, and all benthic fluxes were measured on material that reached the sea floor before February/March of 1998 (Sayles et al., 2001). The estimated burial rates integrate time periods on the order of 1000+ years (Sayles et al., 2001). The emergence of the southern ACC as the zone of maximum $BSiO_2$ flux in all pelagic estimates thus provides evidence that it was the zone of maximum $BSiO_2$ production and export in both 1996–1997 and 1997–1998. The benthic data, which integrate over longer time scales, further imply that those fluxes may have been maximal in the southern ACC quite consistently during the past 1000+ years.

A temporally persistent pattern of the kind described above is exactly what would be expected if the control of $BSiO_2$ production and export is as Sigmon et al. (2002) have proposed. Briefly, they showed that during the spring and summer of 1997–1998 diatoms exported 70–80% of the Si that was available in the upper 50 m at the end of winter, at all latitudes north of 65°S. As a result, $BSiO_2$ export was greatest in the southern ACC, where initial surface-layer $[Si(OH)_4]$ was 35–55 μM, least in the northern ACC where initial concentrations were ~10 μM and intermediate in the intervening gradient region associated with the APF. South of 65°S the initial $[Si(OH)_4]$ in surface waters was >55 μM, but relatively little of that Si was used due to the combined effects of a short ice-free season and possible Fe limitation. Thus annual production and export of $BSiO_2$ are maximal between 59°S and 65°S because they are limited by low late-winter $[Si(OH)_4]$ north of 59°S and by prolonged ice cover and possible Fe limitation south of 65°S. Both of those conditions are persistent features in the Southern Ocean, which are probably not subject to major changes on millennial or shorter time scales. Thus the southern ACC should be the zone of maximum $BSiO_2$ production and export every year. Vertical budgets derived from the several AESOPS data sets combine to suggest that the expected persistent maximum in all Si fluxes in the southern ACC does in fact occur.

3.4. Selective preservation of opal over organic matter

Fig. 4 presents the estimated annual fluxes, expressed as $BSiO_2$/POC flux ratios. Those ratios increase systematically with depth throughout the water column and upper sediments. Estimated on an annual basis, phytoplankton produced $BSiO_2$ and POC in a mole ratio of ~0.1 in the northern ACC, and 0.2–0.4 in the polar frontal region, southern ACC and Ross Gyre. The mean $BSiO_2$/POC ratio measured in pure diatom cultures growing under nutrient-replete conditions is ~0.13 (Brzezinski, 1985). Thus the observed $BSiO_2$/POC production ratios of 0.1–0.4 imply that diatoms accounted for a large fraction of the annual POC production throughout the system, and that those diatoms had unusually high Si/C production ratios in the polar frontal region, southern ACC and Ross Gyre. As also reported by Buesseler et al. (2001), ratios of opal export to POC export from the upper 100 m ranged regionally from 0.2 to 0.6, and the $BSiO_2$/POC ratio increased to 1.5–4.5 in the material reaching 1000 m. The large compositional change between 100 and 1000 m reflects the ~90% remineralization of POC discussed above, while biogenic silica fluxes decreased by only 10–70% (Fig. 3b). POC remineralization continued to a diminished extent in the >1000 m water column, at least in the northern ACC and the polar frontal region, while opal passed from 1000 m to the sea floor without measurable loss. This caused the mole ratio of opal to POC in material delivered to the sea floor to range from 2.2 to 7.6. While 83–95% of the $BSiO_2$ that reached the sea floor dissolved in the upper sediments, 97–99% of the POC reaching the sea floor was remineralized, with the result that the ratio of long-term opal burial to long-term

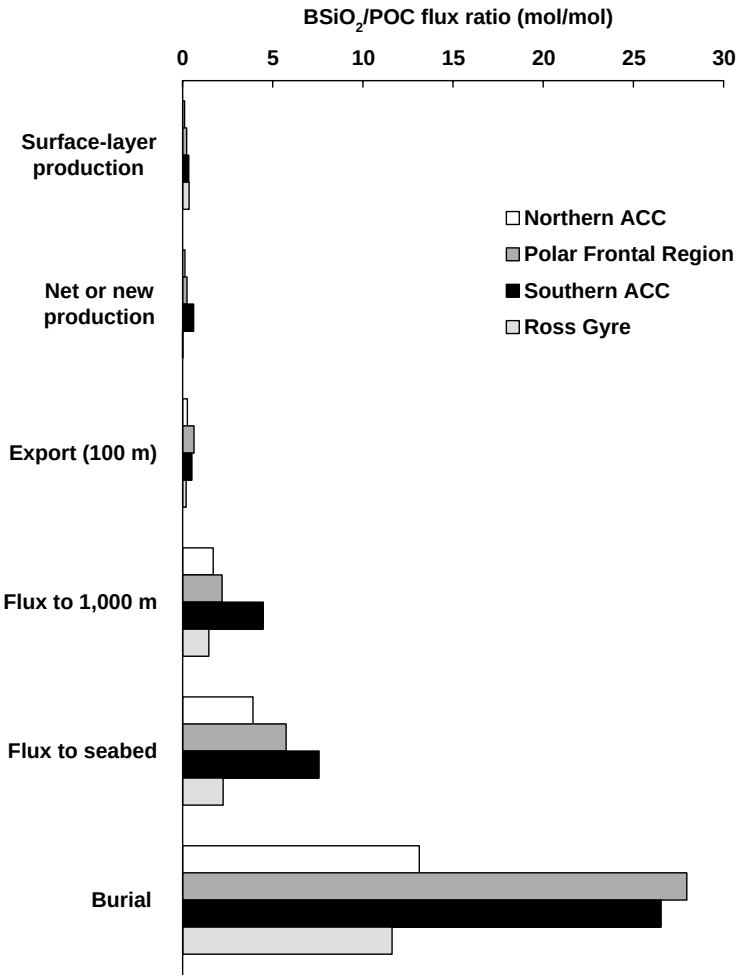

Fig. 4. Annual flux estimates reported in Fig. 3, expressed as $BSiO_2$/POC flux ratios (mol/mol).

POC burial increases to 11.6–28. It is clear from these data that one reason why opal-rich, organic-poor sediments are accumulating beneath the ACC is that the biogenic material produced by phytoplankton is selectively stripped of organic matter at every stage in its passage through the water column and into the seabed. Another reason, as noted by Sayles et al. (2001), is that other sedimentary components such as $CaCO_3$ and terrigenous material accumulate only very slowly in the abyssal sediments of the ACC.

3.5. Comparison of POC and $BSiO_2$ fluxes in the ACC with those in other oceans

POC fluxes. The estimated annual ^{14}C primary productivity in the ACC at 170°W (6.9–8.7 mol $C\,m^{-2}\,yr^{-1}$) is somewhat higher than the mean annual productivity in the ACC south of 55°S estimated from satellite ocean-color and surface irradiance data (Antoine et al., 1996, Behrenfeld and Falkowski, 1997). Subsequent estimates, based on ocean-color data obtained concurrently with our observations (October 1997–September

Table 4
Estimated fluxes of particulate organic carbon and biogenic silica in the Pacific sector of the Sothern Ocean, compared with those in selected other ocean systems.

Region	POC production (mol C m^{-2} y^{-1})	New or export POC production (mol C m^{-2} y^{-1})	POC flux to ~1,000 m (mol C m^{-2} y^{-1})	$BSiO_2$ production (mol Si m^{-2} y^{-1})	Net or export $BSiO_2$ production (mol Si m^{-2} y^{-1})	$BSiO_2$ flux to ~1,000 m (mol Si m^{-2} y^{-1})	Reference(s)
Southern Ocean @ 170°W	6.9 – 8.7	2.1 – 3.8	0.17 – 0.21	0.8 – 3.0	0.3 – 2.4	0.28 – 0.94	This study
Ross Sea shelf [1]	11.9	5.1	0.41[2]	2.0	0.71	0.48[2]	Nelson et al., 1996
Sargasso Sea near Bermuda	9 – 15	2.5 – 2.6	0.08 – 0.13[3]	0.24	0.03 – 0.05	—[4]	Michaels et al., 1994; Nelson & Brzezinski, 1997; Buesseler et al., 2000; W. Deuser, unpublished data
N. Pacific Gyre near Hawaii	12 – 17	0.8	0.1[5]	—[4]	—[4]	0.02	Letelier et al., 1996; Karl et al. 1996; Scharek et al., 1999
Equatorial Pacific	22 – 41	1.8 – 6.3	0.1	—[4]	—[4]	0.12	Barber et al., 1996; McCarthy et al., 1996; Honjo et al., 1995
Arabian Sea	23 – 43	1.0 – 3.4	0.17 – 0.56	—[4]	—[4]	0.2	Honjo et al., 1999; Lee et al., 1998
Global average	10 – 13	2.6	0.2	0.6 – 0.8	0.3 – 0.4	0.15	Antoine et al., 1996; Behrenfeld & Falkowski, 1997; Nelson et al., 1995; Schlitzer, 2000; Honjo, 1997

[1] Shelf-wide mean fluxes reported
[2] Fluxes to sediment traps at 250 m; mean bottom depth of the shelf is 550 m.
[3] Traps were located at 500 and 1500 m; the higher value shown is the flux to 500 m, the lower value the flux to 1500 m.
[4] No data-based estimate is available.
[5] Include carbonate, so overestimates POC flux.

1998) suggest that zonally averaged primary productivity in the ACC ranges from $\sim$2.4 mol C m^{-2} yr^{-1} in seasonally ice-covered waters to $\sim$6 mol C m^{-2} yr^{-1} in the polar frontal region (Moore and Abbott, 2000). Spatially integrated productivity in the polar frontal region and all waters to the south, an area of 3.07×10^7 km^2, was estimated in that study to be 1.42 Pg C yr^{-1} (1 petagram (Pg) = 10^{15} g), a mean productivity of $\sim$46 g C m^{-2} yr^{-1} ($\sim$3.9 mol C m^{-2} yr^{-1}). Those recent estimates remain somewhat lower than our ^{14}C-based estimate for the AESOPS study area, but they are generally within the factor-of-two range that must be exceeded before differences in annual estimates are meaningful. These estimates thus suggest that the annual primary productivity we have estimated at 170°W is close to the circumpolar average for the ACC. The highest recent estimate of primary productivity in the Southern Ocean is 3.2–4.0 Pg C yr^{-1}, integrated for all waters south of 50°S (Arrigo et al., 1998), an area of 4.6×10^7 km^2 (Moore and Abbott, 2000). The regional productivity estimate of Arrigo et al. (1998) thus represents a mean productivity of $\sim$70–90 g C m^{-2} yr^{-1} ($\sim$5.8–7.5 mol C m^{-2} yr^{-1}), which is indistinguishable from our estimate of 6.9–8.7 mol C m^{-2} yr^{-1} for the ACC at 170°W.

While approximately average for the ACC, primary productivity of 6.9–8.7 mol C m^{-2} yr^{-1} is considerably lower than that in most other oceans (Table 4). For example, multi-year records of ^{14}C productivity at the JGOFS Bermuda Atlantic Time Series (BATS) site in the Sargasso Sea range interannually from 9 to 15 mol C m^{-2} yr^{-1} (Michaels et al., 1994) and those at the JGOFS Hawaii Ocean Time-series (HOT) site in the North Pacific Central Gyre from 12 to 17 mol C m^{-2} yr^{-1} (Letelier et al., 1996). Thus our ^{14}C-based productivity estimate in each of three sub-regions of the ACC at 170°W is somewhat lower than ^{14}C-based productivity estimates from the classically oligotrophic subtropical gyres.

^{15}N-based estimates of annual new production and ^{234}Th-based estimates of annual POC export in the four sub-regions of the AESOPS study area range from 1.7 to 3.9 mol C m^{-2} (Table 3a, Fig. 3a). These two independent estimates both indicate that the f ratio (new production/total POC production; Eppley and Peterson, 1979) is $\sim$0.4 on an annual basis throughout the system (Table 3a). These f ratios are significantly higher than those in other open-ocean systems. For example, f ratios are generally $<$0.15 in subtropical gyres (e.g. Eppley and Peterson, 1979; Harrison et al., 1996) and have been estimated to be only 0.04–0.08 in the Arabian Sea (Lee et al., 1998) and 0.02–0.10 in the equatorial Pacific (Buesseler, 1998).

The relatively high f ratios and export efficiencies we observed in the Southern Ocean at 170°W result in annual POC export that is similar to that in more productive systems at lower latitudes, in spite of the lower primary productivity (Table 4). Our estimated export of 1.7–3.8 mol C m^{-2} yr^{-1} in the ACC and Ross Gyre is indistinguishable from the 2.6 mol C m^{-2} yr^{-1} estimated for the Sargasso Sea by Michaels et al. (1994) from seasonal drawdown of dissolved inorganic C and the 2.5 mol C m^{-2} yr^{-1} estimated for that same system by Buesseler et al. (2000) from ^{234}Th deficits and the POC/^{234}Th ratio of the sinking material collected by neutrally buoyant sediment traps. The annual POC export we estimate in the ACC is also similar to that reported in the Arabian Sea, even though annual primary productivity in the Arabian Sea is estimated to be 3–5 times that in the AESOPS study area (Lee et al., 1998; see Table 4).

Eppley and Peterson (1979) noted a large-scale pattern in which f ratios increase with increasing total primary productivity, implying that POC export from eutrophic surface waters should be many times greater than that from oligotrophic systems. However, the relationship presented by Eppley and Peterson was based entirely on data from tropical and subtropical areas, and does not appear to hold in polar oceans of either the northern or southern hemisphere (e.g. Smith and Harrison, 1991). Instead, f ratios in high-latitude systems generally range from $\sim$0.3 to $\sim$0.7, in productive and unproductive regions alike (data from numerous studies, summarized by Nelson, 1992). A consequence of this relationship is that POC export from low-productivity surface waters in polar oceans may be significantly higher than that from low-productivity areas in the tropics or

subtropics. Buesseler (1998) examined this export efficiency throughout the world's oceans and attributes high export efficiency in the polar oceans to diatom-dominated food webs. The AESOPS data are consistent with that high-latitude pattern, with the result that annual new production and POC export in the ACC at 170°W are approximately average for the global ocean despite low primary productivity (Table 4).

Annual POC fluxes to 1000 m ranged from 0.14 to 0.21 mol C m^{-2} (Table 3, Fig. 3a), about twice the global average (Honjo et al., 2000). The carbon budget thus indicates that POC export efficiency is high (remineralization efficiency is low) throughout the upper 1000 m in the ACC. The overall result of this high export efficiency is that, although annual primary productivity is lower than that in most other ocean habitats, annual POC export from surface waters is somewhere near the global average and annual POC flux to the deep ocean is about twice the global average (Table 4).

Opal fluxes. In contrast to the low annual production of POC, estimated annual rates of $BSiO_2$ production are substantially higher in the ACC than in most other oceans (Table 4). The AESOPS data indicate that $BSiO_2$ production in the Pacific sector of the ACC ranges from ~0.8 to 3.0 mol Si m^{-2} yr^{-1} (Fig. 3b). Those rates are 3–12 times the annual $BSiO_2$ production reported at the BATS site, and $BSiO_2$ production in all subregions except the northern ACC is well above the global average of 0.6–0.8 mol Si m^{-2} yr^{-1} (Table 4). High rates of $BSiO_2$ production in surface waters appear to be quite common in the Southern Ocean. Nelson et al. (1996) estimated a mean production of 2.0 mol Si m^{-2} yr^{-1} over the Ross Sea shelf, Pondaven et al. (2000) estimated rates ranging regionally from 1.6 to 3.3 mol Si m^{-2} yr^{-1} in the Indian Ocean sector of the ACC and Rutgers van der Loeff et al. (2002) estimated silica production to be 1.6 mol Si m^{-2} yr^{-1} in the polar frontal region of the Atlantic sector.

Net $BSiO_2$ production and export from the upper 100 m, as estimated from AESOPS data, are also considerably higher in the ACC than that in other oceans (Table 4). The estimated net $BSiO_2$ production (~0.4–2.4 mol Si m^{-2} yr^{-1}) and export (~0.3–1.4 mol Si m^{-2} yr^{-1}) are an order of magnitude greater than at the BATS site and 2–5 times the estimated global mean. As is the case for $BSiO_2$ production, high rates of net $BSiO_2$ production and export appear to be widespread in the Southern Ocean. Net $BSiO_2$ production has been estimated to average 0.7 mol Si m^{-2} yr^{-1} over the Ross Sea shelf (Nelson et al., 1996), to range regionally from 0.7 to 2.3 mol Si m^{-2} yr^{-1} in the Indian Ocean sector of the ACC (Pondaven et al., 2000) and to be 0.4–1.1 mol Si m^{-2} yr^{-1} in the polar frontal region of the Atlantic (Rutgers van der Loeff et al., 2002).

Taken together, the high rates of $BSiO_2$ production and export, low primary productivity and moderate POC export imply that the relationship between the cycles of carbon and silicon in Southern Ocean surface waters is very different from that in other oceans, as was suggested recently by Ragueneau et al. (2000). The ACC is among the most productive, highest-export systems in the ocean with respect to biogenic silica. But for POC, the main form in which biological processes transport carbon to the deep ocean, export in the ACC is only average and primary productivity lower even than that in the mid-ocean gyres.

3.6. Potential causes and implications of Si-enriched, C-depleted primary production and export

The reasons for the observed low rates of POC production with high accompanying rates of $BSiO_2$ production and export in the Southern Ocean are not yet apparent. One clear possibility, however, is the effect of low [Fe] on the elemental composition of diatoms, coupled with the abundant supply of $Si(OH)_4$ to surface waters via upwelling. Studies in several systems, including the Southern Ocean, have shown that Fe deficiency increases the Si/N and Si/C uptake ratios of diatoms by a factor of 2–3 (Hutchins and Bruland, 1998; Takeda, 1998). Fe limitation has been hypothesized to be the main cause of the HNLC character of the Southern Ocean (Martin, 1990), and has now been demonstrated experimentally in several other sectors of the ACC (Van Leeuwe et al., 1997; Boyd et al., 2000). Mixed-layer [Fe]

was consistently <0.3 nM throughout the AESOPS study area (Measures and Vink, 2001), and experiments performed during AESOPS indicate that Si/N uptake ratios were increased by as much as a factor of six under the resulting Fe limitation (Franck et al., 2000). During AESOPS a diatom bloom developed, which was intense enough to deplete surface $[Si(OH)_4]$ from 35–50 μM to <2 μM throughout the entire north–south extent of the southern ACC leading Brzezinski et al. (2001) to conclude that Fe has little effect on the annual yield of siliceous biomass in this region even if Fe limitation slows the rate at which silicic acid is depleted. Primary production, N and P drawdown and new production in this same bloom were modest (Sambrotto and Mace, 2000, Dickson and Orchardo, 2001; Morrison et al., 2001), and Fe deficiency caused Si to be taken up in high proportions to both C and N (Franck et al., 2000). Thus several data sets obtained during AESOPS are consistent with the hypothesis that the observed Si-enriched, C-depleted character of phytoplankton production and particle export in the ACC is a consequence of low Fe availability.

One implication of the above scenario is that low [Fe] limits the annual production and export of organic matter in the Southern Ocean while having little or no effect on the annual production or export of biogenic silica. If so, then selective Fe control of the annual production of organic matter, with no accompanying control of annual $BSiO_2$ production, must be considered in any attempt to reconstruct Southern Ocean paleoproductivity from the opal sediment record. Data records from the Vostok ice core in Antarctica show that each of the last four glacial epochs was characterized by low atmospheric CO_2 (Petit et al., 1999), implying that the biological pumping of CO_2 from the atmosphere to the ocean may have been more efficient during glacial times. It also has been argued, based on Vostok ice core data, that Fe was much more readily available in Southern Ocean surface waters during the last glacial maximum (Martin, 1990). The potential cause-and-effect relationship is obvious: Release from Fe limitation during glacial times would have permitted diatoms to grow with significantly higher N/Si and C/Si ratios. Annual production and export of $BSiO_2$ would not have been significantly higher than they are today, as the available Si in surface water is almost completely used under present conditions (Brzezinski et al., 2001; Sigmon et al., 2002). In contrast, POC production and export would have been at least twice as high, perhaps as much as six times as high, as they are at present. If this reasoning is correct, then POC production and export during glacial times could have been 2–6 times their present values without increasing either the accumulation rate or the opal content of the sediments being generated.

There is little evidence that opal accumulation rates south of the APF were higher during glacial times than they are at present. Some data in fact suggest that those rates were lower during the last glacial maximum (Mortlock et al., 1991; Kumar et al., 1995; Anderson et al. 2002) and that residual silicic acid concentrations in surface waters were higher (De La Rocha et al., 1998). There is, however, a growing body of evidence that the ratio of organic carbon burial to opal burial south of the APF was significantly higher during glacial times. Anderson et al. (2002) have presented sediment core data from the Atlantic sector of the ACC indicating that this ratio was approximately three times higher during each of the past two glacial periods than during the ensuing interglacials. If those changes reflect changes in the ratio of POC export to $BSiO_2$ export from surface waters, then there was approximately three times as much POC export per unit $BSiO_2$ export during each of the last two glacial maxima as there is at present. That difference exactly matches the change in diatom elemental composition that is known to occur when the cells are released from Fe deficiency.

It has recently been suggested that the Southern Ocean was a much stronger sink for atmospheric CO_2 during the last glacial maximum than it is at present, with total POC export 2.9–3.6 Pg C yr^{-1} greater than it is now (Moore et al., 2000). According to those calculations about half of the hypothesized increase in POC export occurred in subantarctic waters north of 55°S, implying increased export of $\sim$1.5–1.8 Pg C yr^{-1} within the ACC proper. The mean POC export we estimate in the ACC south of 55°S at 170°W is

2.5 mol C m^{-2} yr^{-1} (Table 3). Extrapolating that export to the area of the ACC (3.3×10^7 km^2; Tréguer and Jacques, 1992) yields an estimated present export of 8.3×10^{13} mol C yr^{-1} (~ 1.0 Pg C yr^{-1}) in the region. Thus if POC export in the ACC was 1.5–1.8 Pg C yr^{-1} higher during the last glacial maximum as hypothesized by Moore et al., it would have been approximately 2.5–2.8 Pg C yr^{-1}, or 2.5–2.8 times its present value. As we calculated above, POC export could have been increased by almost exactly that amount, with no corresponding increase in opal export, if diatoms were permitted to grow with the normal elemental composition characteristic of Fe-replete conditions.

Acknowledgements

We thank the crews of the *Nathaniel B. Palmer* and *Roger Revelle* for excellent support during the seagoing phase of this study. Many people assisted us either at sea or during the later analysis of samples and data, including John Andrews, Julie Arrington, Larry Ball, Cal Eck, Alan Fleer, Martin Fleisher, Valerie Franck, Zev Frankel, Bill Golden, Joanne Goudreau, Dave Hirschberg, Janice Jones, Bonnie Mace, Steve Manganini, Chris Moser, Joe Orchardo and Cara Sucher. We particularly thank Michael Bacon, Michael Bender, J. Kirk Cochran, Werner Deuser, Jack Dymond and Chris Measures for providing access to unpublished data, and for advice on the general issues dealt with in this paper. Gerhard Fischer provided comments and insights on an earlier version of this paper, which were particularly helpful. This work was sponsored by the US National Science Foundation through grants OPP-9530677, OCE-9911312, OPP-9614028 and OCE-9530688 to Oregon State University, OPP-9531982 to the University of California, OPP-9531981 to Duke University, OPP-9530379, OPP-9530398 OCE-9530981, OCE-9819151 and OPP-9530611 to Columbia University, OPP-9530746 to the University of Rhode Island and OPP-9530861, OPP-9530300 and OCE-9530719 to the Woods Hole Oceanographic Institution. This is US JGOFS contribution #670.

References

Anderson, R.F., Chase, Z., Fleisher, M.Q., Sachs, J., 2002. The southern ocean's biological pump during the last glacial maximum. Deep-Sea Research Part II 49, 1909–1938.

Antoine, D., André, J.-M., Morel, A., 1996. Oceanic primary production 2. Estimation at global scale from satellite (coastal zone color scanner) chlorophyll. Global Biogeochemical Cycles 10, 57–69.

Arrigo, K.R., Worthen, D., Schnell, A., Lizotte, M.P., 1998. Primary production in Southern Ocean waters. Journal of Geophysical Research 103, 15587–15600.

Banse, K., 1996. Low seasonality of low concentrations of surface chlorophyll in the subantarctic water ring: underwater irradiance, iron or grazing? Progress in Oceanography 37, 241–291.

Barber, R.T., Sanderson, M.P., Lindley, S.T, Chai, F., Newton, J., Trees, C.C., Foley, D.G., Chavez, F.P., 1996. Primary productivity and its regulation in the equatorial Pacific during and following the 1991–92 El Niño. Deep-Sea Research Part II 43, 933–969.

Barth, J.A., Cowles, T.J., Pierce, S.D., 2001. Mesoscale frontal and bio-optical structure of the antarctic polar front near 170°W during spring. Journal of Geophysical Research 106, 13879–13902.

Bathmann, U.V., Scharek, R., Klaas, C., Dubischar, C.D., Smetacek, V., 1997. Spring development of phytoplankton biomass and composition in major water masses of the Atlantic sector of the Southern Ocean. Deep-Sea Research Part II 44, 51–68.

Behrenfeld, M.J., Falkowski, P.G., 1997. Photosynthetic rates derived from satellite-based chlorophyll concentration. Limnology and Oceanography 42, 1–20.

Bender, M., Grande, K., Johnson, K., Marra, J., Williams, P.J.leB., Sieburth, J., Pilson, M., Langdon, C., Hitchcock, G., Heinemann, C., 1987. A comparison of four methods for the determination of planktonic community metabolism. Limnology and Oceanography 32, 1085–1098.

Bender, M., Orchardo, J., Dickson, M.-L., Barber, R., Lindley, S., 1999. In vitro O_2 fluxes compared with ^{14}C production and other rate terms during the JGOFS Equatorial Pacific experiment. Deep-Sea Research Part II 46, 637–654.

Boyd, P.W., Watson, A.J., Law, C.S., Abraham, E.R., Trull, T., Murdoch, R., Bakker, D.C.E., Bowie, A.R., Buesseler, K.O., Chang, H., Charette, M., Croot, P., Downing, K., Frew, R., Gall, M., Hadfield, M., Hall, J., Harvey, M., Jameson, G., LaRoche, J., Liddicoat, M., Ling, R., Maldonado, M.T., McKay, M.M., Nodder, S., Pickmore, S., Pridmore, R., Rintoul, S., Safi, K., Sutton, P., Strzepek, R., Tanneberger, K., Turner, S., Waite, A., Zeldis, J., 2000. A mesoscale phytoplankton bloom in the polar Southern Ocean stimulated by iron fertilization. Nature 407, 695–702.

Broecker, W.S., Peng, T.-H., 1982. Tracers in the Sea. Eldigio Press, Palisades, New York, 690pp.

Brown, S.G., Lockyer, C.H., 1984. Whales. In: Laws, R.M. (Ed.), Antarctic Ecology. Academic Press, London, pp. 717–781.

Brzezinski, M.A., 1985. The Si:C:N ratio of marine diatoms interspecific variability and the effect of some environmental variables. Journal of Phycology 21, 347–357.

Brzezinski, M.A., Nelson, D.M., Franck, V.M., Sigmon, D.E., 2001. Silicon dynamics within an intense open-ocean diatom bloom in the pacific sector of the southern ocean. Deep-Sea Research Part II 48, 3997–4018.

Buesseler, K.O., 1998. The decoupling of production and particulate export in the surface ocean. Global Biogeochemical Cycles 12 (2), 297–310.

Buesseler, K.O., Bacon, M.P., Cochran, J.K., Livingston, H.D., 1992. Carbon and nitrogen export during the JGOFS north Atlantic bloom experiment estimated from ^{234}Th:^{238}U disequilibria. Deep-Sea Research Part I 39 (7/8), 1115–1137.

Buesseler, K.O., Ball, L., Andrews, J., Benitez-Nelson, C., Belastock, R., Chai, F., Chao, Y., 1998. Upper ocean export of particulate organic carbon in the Arabian Sea derived from thorium-234. Deep-Sea Research Part II 45 (10–11), 2461–2487.

Buesseler, K.O., Steinberg, D.K., Michaels, A.F., Johnson, R.J., Andrews, J.A., Valdes, J.R., Price, J.F., 2000. A comparison of the quantity and composition of material caught in neutrally buoyant versus surface-tethered sediment traps. Deep-Sea Research Part I 47, 277–294.

Buesseler, K.O., Ball, L., Andrews, J., Cochran, J.K., Hirschberg, D.J., Bacon, M.P., Fleer, A., Brzezinski, M., 2001. Upper ocean export of particulate organic carbon and biogenic silica in the southern ocean along 170°W. Deep-Sea Research Part II 48, 4247–4273.

Chase, Z., 2001. Trace elements as regulators (Fe) and recorders (U, Pa, Th, Be) of biological productivity in the ocean. Ph.D. Thesis, Columbia University.

Croxall, J.P., Prince, P.A., 1979. Antarctic seabird and seal monitoring studies. Polar Record 19, 573–595.

De La Rocha, C.L., Brzezinski, M.A., DeNiro, M.J., Shemesh, A., 1998. Silicon-isotope composition of diatoms as an indicator of past oceanic change. Nature 395, 680–683.

DeMaster, D.J., 1981. The supply and accumulation of silica in the marine environment. Geochimicha et Cosmochimica Acta 45, 1715–1732.

DeMaster, D.J., 2002. Continental margin biogenic silica accumulation: coupling of the marine cycles of organic matter and biogenic silica. Deep-Sea Research Part II, submitted.

DeMaster, D.J., Nelson, T.M., Harden, S.L., Nittrouer, C.A., 1991. The cycling and accumulation of biogenic silica and organic carbon in antarctis deep-sea and continental margin environments. Marine Chemistry 35, 489–502.

Dickson, M.-L., Orchardo, J., 2001. Oxygen production, respiration in the antarctic polar front region during austral spring and summer. Deep-Sea Research Part II 48, 4275–4297.

El-Sayed, S.Z., 1978. Primary productivity and estimates of potential yields of the Southern Ocean. In: McWhinnie, M.A. (Ed.), Polar Research. Westview Press, New York, pp. 141–160.

El-Sayed, S.-Z., Turner, J.T., 1975. Productivity of the Antarctic and tropical/subtropical regions: a comparative study. In: Dunbar, M. (Ed.), Polar Oceans. Arctic Institute of North America, Montreal, pp. 463–503.

Eppley, R.W., Peterson, B.J., 1979. Particulate organic matter flux and planktonic new production in the deep ocean. Nature 282, 677–680.

Franck, V.M., Brzezinski, M.A., Coale, K.H., Nelson, D.M., 2000. Iron and silicic acid availability regulate Si uptake in the Pacific sector of the Southern Ocean. Deep-Sea Research Part II 47 (15–16), 3315–3338.

Francois, R., Bacon, M., Suman, D.O., 1990. Thorium-230 profiling in deep-sea sediments: high-resolution records of flux and dissolution of carbonate in the equatorial Atlantic during the last 24,000 years. Paleoceanography 5 (5), 761–787.

Goodell, H.G., Houtz, R., Ewing, M., Hayes, D., Naini, B., Echols, R.J., Kennett, J.R., Donahue, J.G., 1973. Marine Sediments of the Southern Oceans. Antarctic Map Folio Series, Folio 17, American Geographic Society.

Gordon, A.L., Molinelli, .E.J., 1986. Thermohaline and chemical distributions and the Atlas data set. In: Gordon, A.L. (Ed.), Southern Ocean Atlas. Columbia University Press, New York, pp. 3–233.

Harrison, W.G., Harris, L.R., Irwin, B.D., 1996. The kinetics of nitrogen utilization in the oceanic mixed layer: nitrate and ammonium interactions at nanomolar concentrations. Limnology and Oceanography 41, 16–32.

Henderson, G.M., Heinze, C., Anderson, R.F., Winguth, M.E., 1999. Global distribution of the ^{230}Th flux to ocean sediments constrained by GCM modelling. Deep-Sea Research Part I 46, 1861–1893.

Holm-Hansen, O., El-Sayed, S.-Z., Franceschini, G.S., Cuhel, R.L., 1977. Primary production and factors controlling phytoplankton growth in the Southern Ocean. In: Llano, G. (Ed.), Adaptations within Antarctic Ecosystems. Gulf Publishing Co., Houston, pp. 11–50.

Honjo, S., 1997. The rain of ocean particles and earth's carbon cycle. Oceanus 40, 4–7.

Honjo, S., Dymond, J., Collier, R., Manganini, S., 1995. Export production of particles to the interior of Equatorial Pacific Ocean during 1992 Eq. Pac. experiment. Deep-Sea Research Part II 42 (2/3), 831–870.

Honjo, S., Dymond, J., Prell, W., Ittekot, V., 1999. Monsoon-controlled export fluxes to the interior of the Arabian Sea: US JGOFS 1994–1995 experiment. Deep-Sea Research Part II 46 (8–9), 1859–1902.

Honjo, S., François, R., Manganini, S., Dymond, J., Collier, R., 2000. Particle fluxes to the interior of the Southern Ocean in the Western Pacific sector along 170°W. Deep-Sea Research Part II 47 (15–16), 3521–3548.

Hutchins, D.A., Bruland, K.W., 1998. Iron-limited diatom growth and Si:N uptake ratios in a coastal upwelling regime. Nature 393, 561–564.

Jenkins, W.J., Goldman, J.C., 1985. Seasonal oxygen cycling and primary production in the Sargasso Sea. Journal of Marine Research 43, 465–491.

Jennings Jr., J.C., Gordon, L.I., Nelson, D.M., 1984. Nutrient depletion indicates high primary productivity in the Weddell Sea. Nature 308, 51–54.

Knox, F., McElroy, M., 1984. Changes in atmospheric CO_2: influence of marine biota at high latitudes. Journal of Geophysical Research 89, 4629–4637.

Kumar, N., Anderson, R.F., Mortlock, R.A., Froelich, P.N., Kubik, P.W., Dittrich-Hannen, B., Suter, M., 1995. Iron fertilization of glacial-age Southern Ocean productivity. Nature 378, 675–680.

Laubischer, R.K., Perissinotto, R., McQuaid, C.D., 1993. Phytoplankton production and biomass at frontal zones in the Atlantic sector of the Southern Ocean. Polar Biology 13, 471–481.

Laws, E.A., 1991. Photosynthetic quotients, new production, net community production in the open ocean. Deep-Sea Research Part I 38, 143–167.

Laws, E.A., Landry, M.R., Barber, R.T., Campbell, L., Dickson, M.-L., Marra, J., 2000. Carbon cycling in primary production bottle incubations: inferences from grazing experiments and photosynthetic studies using ^{14}C and ^{18}O in the Arabian Sea. Deep-Sea Research Part II 47, 1339–1352.

Lee, C., Murray, D.W., Barber, R.T., Buesseler, K.O., Dymond, J., Hedges, J.I., Honjo, S., Manganini, S.J., Marra, J., Moser, C., Peterson, M.L., Prell, W.L., Wakeham, S.G., 1998. Particulate organic carbon fluxes: compilation of results from the 1995 US JGOFS Arabian Sea process study. Deep-Sea Research Part II 45, 2489–2501.

Letelier, R.M., Dore, J.E., Winn, D.D., Karl, D.M., 1996. Seasonal and interannual variations in photosynthetic carbon assimilation at Station ALOHA. Deep-Sea Research Part II 43, 467–490.

Lieth, H., 1975. Historical survey of primary productivity research. In: Lieth, H., Whittaker, R.H. (Eds.), Primary Productivity of the Biosphere. Springer, New York, pp. 7–16.

Longhurst, A.R., Harrison, W.G., 1989. The biological pump: profiles of plankton production and consumption in the upper ocean. Progress in Oceanography 22, 47–123.

Louanchi, F., Najjar, R.G., 2000. A global monthly climatology of phosphate, nitrate and silicate in the upper ocean: spring–summer export production and shallow remineralization. Global Biogeochemical Cycles 14, 957–977.

Martin, J.H., 1990. Glacial–interglacial CO_2 change: the iron hypothesis. Paleoceanography 5, 1–13.

Martin, J.H., Knauer, G.A., Karl, D.M., Broenkow, W.W., 1987. VERTEX: carbon cycling in the northeast pacific. Deep-Sea Research Part 1 34, 267–285.

McCarthy, J.J., Garside, C., Nevins, J.L., Barber, R.T., 1996. New production along 140°W in the equatorial Pacific during and following the 1992 El Niño event. Deep-Sea Research Part II 43, 1065–1093.

Measures, C.I, Vink, S., 2001. Dissolved fe in the upper waters of the pacific sector of the southern ocean. Deep-Sea Research Part II 48, 3913–3941.

Michaels, A.F., Bates, N.R., Buesseler, K.O., Carlson, C.A., Knap, A.H., 1994. Carbon-cycle imbalances in the Sargasso Sea. Nature 372, 537–540.

Moore, J.K., Abbott, M.R., 2000. Phytoplankton chlorophyll distributions and primary production in the Southern Ocean. Journal of Geophysical Research 105, 28709–28722.

Moore, J.K., Abbott, M.A., Richman, J.G., 1999. Location and dynamics of the Antarctic Polar Front from satellite sea surface temperature data. Journal of Geophysical Research 104, 3059–3073.

Moore, J.K., Abbott, M.A., Richman, J.G., Nelson, D.M., 2000. The Southern Ocean at the last glacial maximum: a strong sink for atmospheric CO_2. Global Biogeochemical Cycles 14 (1), 455–475.

Morrison, J.M., Gaurin, S., Codispoti, L.A., Takahashi, T., Millero, F.J., Gardner, W.D., Richardson, M.J., 2001. Seasonal evolution of the hydrographic properties in the Antarctic Circumpolar Current at 170°W during 1997–1998. Deep-Sea Research Part II 48, 3943–3972.

Mortlock, R.A., Charles, C.D., Froelich, P.N., Zibello, M.A., Saltzman, J., Hays, J.D., Burckle, L.H., 1991. Evidence for lower productivity in the Antarctic Ocean during the last glaciation. Nature 351, 220–223.

Nelson, D.M., 1992. Biogeochemical cycles of organic and siliceous matter in the Southern Ocean. In: Gallardo, V.A., Ferreti, O., Moyano, H.I. (Eds.), Oceanografia in Antartide. ENEA-Progetto Antartide, Italia/Centro EULA, Universidad de Concepción, Chile, pp. 9–21.

Nelson, D.M., Brzezinski, M.A., 1997. Diatom growth and productivity in an oligotrophic midocean gyre: a 3-yr record from the Sargasso Sea near Bermuda. Limnology and Oceanography 42, 473–486.

Nelson, D.M., Tréguer, P., Brzezinski, M.A., Leynaert, A., Quéguiner, B., 1995. Production and dissolution of biogenic silica in the ocean: revised global estimates, comparison with regional data and relationship to biogenic sedimentation. Global Biogeochemical Cycles 9, 359–372.

Nelson, D.M., DeMaster, D.J., Dunbar, R.B., Smith Jr., W.O., 1996. Cycling of organic carbon and biogenic silica in the Southern Ocean: estimates of water-column and sedimentary fluxes on the Ross Sea continental shelf. Journal of Geophysical Research 101, 18519–18532.

Nelson, D.M., Brzezinski, M.A., Sigmon, D.E., Franck, V.M., 2001. A seasonal progression of si limitation in the pacific sector of the southern ocean. Deep-Sea Research Part II 48, 3973–3995.

Orsi, A.H., Whitworth, T., Worth, N., 1995. On the meridional extent and fronts of the Antarctic Circumpolar Current. Deep Sea Research Part I 42, 641–673.

Petit, J.R., Jouzel, J., Raynaud, R., Barkov, N.I., Barnola, J.-M., Basile, I., Bender, M., Chapellaz, J., Davis, M., Delaygue, G., Delmotte, M., Kotlyakov, V.M., Legrand, M., Lipenkov, V.Y., Lorius, C., Pépin, L., Ritz, C., Saltzman, E., Stievenard, M., 1999. Climate and atmospheric history of the past 420,000 years from the Vostok ice core, Antarctica. Nature 399, 429–436.

Pondaven, P., Ragueneau, O., Tréguer, P., Hauvespre, A., Dezileau, L., Reyss, J.L., 2000. Resolving the "opal paradox" in the Southern Ocean. Nature 405, 168–172.

Ragueneau, O., Tréguer, P., Leynaert, A., Anderson, R.F., Brzezinski, M.A., DeMaster, D.J., Dugdale, R.C., Dymond, J., Fishcher, G., François, R., Heinze, C., Maier-Reimer, E., Martin-Jézéquel, V., Nelson, D.M., Quéguiner, B., 2000. A review of the Si cycle in the modern ocean: recent progress and missing gaps in the application biogenic opal as a paleoproductivity proxy. Global and Planetary Change 26 (4), 315–366.

Redfield, A.C., Ketchum, B.H., Richards, F.A., 1963. The influence of organisms on the composition of seawater. In: Hill, M.N. (Ed.), The Sea., Vol. 2. Wiley, Interscience, New York, pp. 26–77.

Rutgers van der Loeff, M.M., Buesseler, K.O., Bathmann, U., Hense, I., Andrews, J., 2002. Steady summer production and a sudden spring bloom make a comparable contribution to carbon and opal export near the Antarctic Polar Front, SE Atlantic. Deep-Sea Research Part II, in press.

Sambrotto, R.N., 2001. Nitrogen production in the northern Arabian Sea during the spring intermonsoon and southwest Monsoon seasons. Deep-Sea Research Part II 48 (6–7), 1173–1198.

Sambrotto, R.N., Mace, B.J., 2000. Coupling of biological and physical regimes across the Antarctic Polar Front as reflected by nitrogen production and recycling. Deep-Sea Research Part II 47 (15–16), 3339–3368.

Sarmiento, J.L., Hughes, T.M.C., Stouffer, R.J., Manabe, S., 1998. Simulated response of the ocean carbon cycle to anthropogenic climate warming. Nature 393, 245–252.

Sayles, F.L., Martin, W.R., Chase, Z., Anderson, R.F., 2001. Benthic remineralization and burial of biogenic SiO_2, $CaCO_3$ organic carbon and detrital material in the southern ocean along a transect at. Deep-Sea Research Part II 48, 4323–4383.

Schlitzer, R., 2000. Applying the adjoint method for biogeochemical modeling: export of particulate organic matter in the World Ocean. Geophysical Monographs 114, 107–124.

Scholten, J.C., Fietzke, J., Vogler, S., Rutgers van der Loeff, M., Mangini, A., Koeve, W., Waniek, J., Stoffers, P., Antia, A., Kuss, J., 2001. Trapping efficiencies of sediment traps from the deep eastern North Atlantic: the ^{230}Th calibration. Deep-Sea Research Part II 48 (10), 2383–2408.

Sigmon, D.E., Nelson, D.M., Brzezinski, M.A., 2002. The si cycle in the pacific sector of the southern ocean: seasonal diatom production in the surface layer and export to the deep sea. Deep-Sea Research Part II 49, 1747–1763.

Smith, W.O., Harrison, W.G., 1991. New production in polar regions: the role of environmental controls. Deep-Sea Research Part I 38, 1463–1479.

Smith, W.O., Keene, N.K., Comiso, J.C., 1988. Interannual variability in estimated primary productivity of the Antarctic marginal ice zone. In: Sahrhage, D. (Ed.), Antarctic Ocean and Resources Variability. Springer, Berlin, pp. 131–139.

Smith Jr., W.O., Anderson, R.F., Moore, J.K., Codispoti, L.A., Morrison, J.M., 2000. The US Southern Ocean Joint Global Ocean Flux Study: an introduction to AESOPS. Deep-Sea Research Part II 47 (15–16), 3073–3093.

Suman, D.O., Bacon, M.P., 1989. Variations in Holocene sedimentation in the North-American basin determined from Th-230 measurements. Deep-Sea Research Part I 36 (6), 869–878.

Takeda, S., 1998. Influence of iron availability on nutrient consumption ratio of diatoms in oceanic waters. Nature 393, 774–777.

Tréguer, P., Jacques, G., 1992. Dynamics of nutrients and phytoplankton, and fluxes of carbon, nitrogen and silicon in the Antarctic Ocean. Polar Biology 12, 149–162.

Tréguer, P., Nelson, D.M., Van Bennekom, A.J., DeMaster, D.J., Leynaert, A., Quéguiner, B., 1995. The silica balance in the world ocean: a re-estimate. Science 268, 375–379.

Van Bennekom, A.J., Berger, G.W., van der Gast, S.J., Devries, R.T., 1988. Primary productivity and the silica cycle in the Southern Ocean (Atlantic sector). Paleogeography, Paleoclimatology and Paleoecology 67, 19–30.

Van Leeuwe, M.A., Scharek, R., De Baar, H.J.W., De Jong, J.T.M., Goeyens, L., 1997. Iron enrichment experiments in the Southern Ocean: physiological responses of plankton communities. Deep-Sea Research Part II 44, 189–208.

Volk, T., Hoffert, M.I., 1985. Ocean carbon pumps: analysis of relative strengths and efficiencies in ocean-driven atmospheric CO_2 changes. In: Sundquist, E.T., Broecker, W.S. (Eds.), The Carbon Cycle and Atmospheric CO_2: Natural Variations Archean to Present. American Geophysical Union, Washington, pp. 99–110.

Yu, E.-F., Francois, R., Bacon, M.P., Honjo, S., Fleer, A.P., Manganini, S.J., Rutgers van der Loeff, M.M., Ittekot, V., 2001. Trapping efficiency of bottom-tethered sediment traps estimated from the intercepted fluxes of ^{230}Th and ^{231}Pa. Deep-Sea Research Part I 48, 865–889.